**AN ABSTRACT OF THE THESIS OF**

William R. Brassfield for the degree of Master of Science in Electrical and Computer Engineering presented on March 31, 1993.

Title: Direct Torque Control for Brushless Doubly-Fed Machines



Abstract approved: _____, (Rene Spee

The Brushless Doubly-Fed Machine (BDFM) has recently become an important research topic in the field of variable-speed AC drives. In recent studies, the BDFM has shown significant potential for improving the reliability and performance of AC drive systems, as well as reducing total system cost. While the BDFM offers several advantages over existing AC drives in steady-state operation, it suffers from dynamic instabilities and slow response times, and a feedback control system is necessary. The mathematics of the BDFM are much more complicated than those of a singly-fed machine, and thus traditional control methods can't be applied. In this thesis, a control method known as "Direct Torque Control" has been adapted from that of a singly-fed induction machine and successfully applied to the BDFM.

The thesis begins by discussing the background of the BDFM, its open-loop operating characteristics, and some of the control considerations. The reduced-order system differential equations are introduced, and it is noted that they are coupled and nonlinear. Furthermore, all state variables are time-varying (but periodic), even in steady-state operation. In the controller development, it is found that a linear relationship exists between the desired torque/flux-level change and the d-q voltages

to be applied to the control winding of the machine via the power-electronic converter. This linear relationship, together with a one-step-ahead predictor to compensate for computational delay, is successfully used to control the speed and efficiency of the machine, for a wide range of speeds and load torques. Numerous open- vs. closed-loop simulations are compared and summarized, and it is found that the performance of the BDFM is greatly improved in the closed-loop, with faster response and reduced oscillation. Further simulations investigating the robustness of the controller are summarized, and it is found that the controller is reasonably insensitive to errors in most of the the static machine parameters. Hardware implementation is briefly discussed but is not complete; laboratory results are not yet available but should be soon. Future controller considerations are then discussed; included among the recommendations are an on-line parameter estimator for use in adaptive control, and a controller for generator applications of the BDFM.

# Direct Torque Control
# for
# Brushless Doubly-Fed Machines

by

William R. Brassfield

A THESIS

submitted to

Oregon State University

in partial fulfillment of
the requirements for the
degree of

Master of Science

Completed March 31, 1993

Commencement June 1993

APPROVED:

Redacted for Privacy

Assistant Professor of Electrical and Computer Engineering
in charge of major

Redacted for Privacy

Head of Department of Electrical and Computer Engineering

Redacted for Privacy

Dean of Graduate School

Date thesis is presented March 31, 1993

Typed by William R. Brassfield

## ACKNOWLEDGEMENTS

Many thanks to all who have provided me with valuable financial support during this research project. Among those who deserve thanks are Boeing, Chevron, and Outstanding College Students of America for their generous graduate fellowship support. Also, I extend many thanks to the Electrical and Computer Engineering Department, for providing me with teaching and research positions and stipends. Finally, many thanks go to Eta Kappa Nu Electrical Engineering Honors Society and Tau Beta Pi Engineering Honors Society for providing recognition and leadership experience. It is their recognition which has made many if not all of my financial rewards possible.

I wish to thank all who have provided me with their time and moral support while working on this thesis. First, I would like to thank Professor Rene Spee, my major professor, for spending numerous hours with me on this project. He has helped me to find my direction when I was lost, he has provided me with useful advice whenever I had questions and needed suggestions, and he has provided me with valuable opportunities to meet with successful, professional people. Most of all, I wish to thank Prof. Spee for his patience in seeing me through my hard times.

Next, I would like to thank the other members of my thesis committee for spending their valuable time reviewing my thesis and providing helpful suggestions. I wish to personally thank Professor Alan Wallace for his supportiveness and willingness to to help me in my times of need. I also extend generous thanks to Professors Ron Mohler and David McIntyre for their willingness to take time out of their busy schedules to participate in this important event.

I wish to thank all of the wonderful professors I have had for my graduate and undergraduate classes. They have taught me a great deal, not only in terms of knowledge, but in terms of professionalism. Some have

been more than just teachers and have been excellent friends, sometimes spending numerous hours in casual, friendly conversation on all topics. These people include (but are not necessarily limited to) Professors Rene Spee, Alan Wallace, and John Saugen (retired). I also want to thank our ECE technician, Ken McCracken for his friendship (and hard work).

I wish to thank my peers on the BDFM Research Team for their support and advice. I give Mohamed (Arif) Salim my special thanks for rooming with me and supporting me at the 1992 IEEE-IAS Conference in Houston, Texas. As his former TA, I also want to thank him for being a highly motivated student who always excelled in the quality and professionalism of his work, and I wish him well in his upcoming thesis defense. I also wish to thank Ashok Ramchandran and Virendra Javadekar for being valuable references, as well as Tom Habetler and Ruqi Li, whose work provided the foundation for this thesis. Also, much thanks to Julian Brent Sessions, who helped me with the assembly programming of the simulator program, doubling its speed and saving countless hours of time.

I wish to also thank my many non-engineering peers in the Campus Ambassadors Campus Ministry, who have provided me with wonderful emotional and spiritual support during my endeavor. Among them are Bob Cole, Steve Barnett, James Hoekema, David Goodwin, Mark Descalzo, Adam Lund, Jonathan Johnson, and our group leader, Jeff Harris. I also send my thanks to Randy Heffner, John Moa, and Mike Thorne for introducing me to the Lord.

I wish to thank my two best friends, Jon Johnson and Adam Kreindel, for providing countless hours of recreational companionship on my "much needed" (and therapeutic) National Parks voyages in the last two years, as well as in many other activities. Without them, I probably would have gone mad; they provided me the means to never forget how beautiful the world really is, in the midst of all the numbers, formulas, and computer code. We have driven, flown, and hiked many thousands of miles together.

Finally, I wish to thank my family for providing both moral and financial support during my years at school. First and foremost, I wish to thank my paternal grandparents, William H. and Barbara M. Brassfield, who raised me since the age of 7 and provided for my college fund. My grandfather deserves special thanks for getting me interested in electrical engineering and mathematics at an early age. He was always there for me, to answer even the toughest questions patiently and in detail. I also wish to thank my aunt and uncle, Donna and Bob Bernardy, for their support, as well as my 3rd-cousins, Jean and Ernie Louvring.

## TABLE OF CONTENTS

## LIST OF FIGURES

## LIST OF TABLES

## LIST OF APPENDICES TABLES

# Direct Torque Control For Brushless Doubly-Fed Machines

# Chapter 1

# Introduction

## 1.1 Background

Although the idea of the BDFM (Brushless Doubly-Fed Machine) has been around for about 80 years [1,2,3], only recently has it been developed for use with a power-electronic converter. The BDFM has two sets of stator coils, one of which is energized directly from the 60 Hz power grid; the other is energized with variable voltage and frequency from a power converter (refer to Figure 1.1). The rotor is of a modified squirrel-cage design; its conductors are cast rather than wound, and hence it has no brushes for excitation. The behavior of the BDFM, in its desired mode of operation, is that of a variable-speed synchronous machine. In the synchronous mode, the rotor speed is solely determined by the frequencies of the stator excitations and is thus independent of load torque. The ability to operate in the synchronous mode distinguishes the BDFM from induction motor drives.

For the sake of future reference, a BDFM based on a 6-pole, 2-pole stator structure and a 4-pole rotor structure shall be used in all discussions throughout this thesis. This configuration also forms the basis of the controller design in this project. It should be noted that other pole structures do exist for the BDFM, and that all such machines operate on the same principle. The system differential equations and controller designs for such machines will all have a similar form; the main differences between such machines are in the speed ranges over which

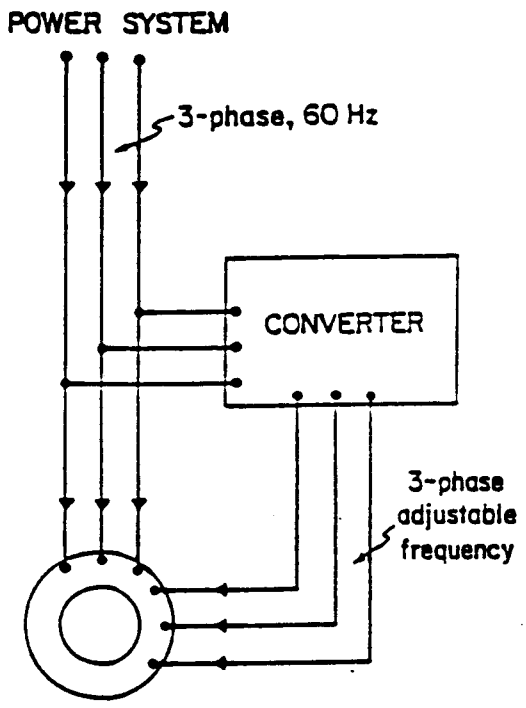


Figure 1.1: BDFM System

they operate, their torque-speed profiles, and the kVA rating of the power converter.

The BDFM studied here is excited directly from the 60 Hz, 3-phase power grid on its 6-pole set of windings. This is where the majority of the power for the machine is to come from. The 2-pole set of windings is used for speed control and is fed from a variable frequency, variable voltage power converter which can produce -60 Hz to 60 Hz output. (Negative frequencies are positive sequence (abc); positive frequencies are negative sequence (acb).) The two rotating magnetic fields of the 6-pole and 2-pole windings interact with the rotor through mutual coupling, and with the rotor's 4-pole structure, a net torque is produced, causing the rotor to spin at a synchronous speed of

$$\omega_r = \frac{60(f_6 - f_2)}{(P_p + P_c)} \quad \text{r/min} \qquad (1.1)$$

In this particular machine, $P_p = 3$, and $P_c = 1$, so this equation becomes

$$\omega_r = 15(f6 - f2) \quad r/min \tag{1.2}$$

Hence, the speed range of the machine is 0 r/min to 1800 r/min, with a midpoint of 900 r/min, which is achieved with DC excitation on the 2-pole winding. Table 1.1 illustrates the relationship between 2-pole frequency and rotor speed.

Table 1.1: Rotor Speed vs. 2-Pole Frequency

| $f_2$, Hz | $\omega_r$, r/min |
|---|---|
| -60 | 1800 |
| -40 | 1500 |
| -20 | 1200 |
| 0 | 900 |
| 20 | 600 |
| 40 | 300 |
| 60 | 0 |

## 1.2 Operating Characteristics

The BDFM has several advantages over conventional types of AC drives. First, as the name of the machine implies, the BDFM has no brushes for rotor excitation. This greatly reduces maintenance costs and increases reliability, especially in applications where the AC drive (or alternator) is physically difficult to access, as in a submersible pump or a windmill generator. Second, the power converter size requirement for the BDFM is less than that of a conventional AC drive because only part of the machine power requirement is processed, rather than all of it. This has tremendous cost-reducing potential because the power converter is typically the most expensive part of an AC drive system, often five times the cost of the motor itself. Third, the BDFM has a wide operating range in terms of speed and torque. The torque-producing ability of the machine is high at very low speeds (near standstill) as well as at full speed (1800 RPM). Finally, the efficiency of the BDFM can potentially rival that of conventional AC drives available.

There are a few disadvantages to the BDFM which should be mentioned here for the sake of fairness and completeness. First, the stator and rotor design for the BDFM are more complicated than that for a singly-fed machine. The stator must be designed to accomodate two sets of coils instead of just one. Second, the BDFM isn't entirely open-loop stable. Narrow speed bands exist, over which the BDFM will not operate synchronously; instead, the speed oscillates around the desired operating point. Third, the BDFM has a cusp-shaped torque-limit envelope, shown in Figure 1.2. This is based on steady-state information and does not include some of the dynamic instabilities of the machine.

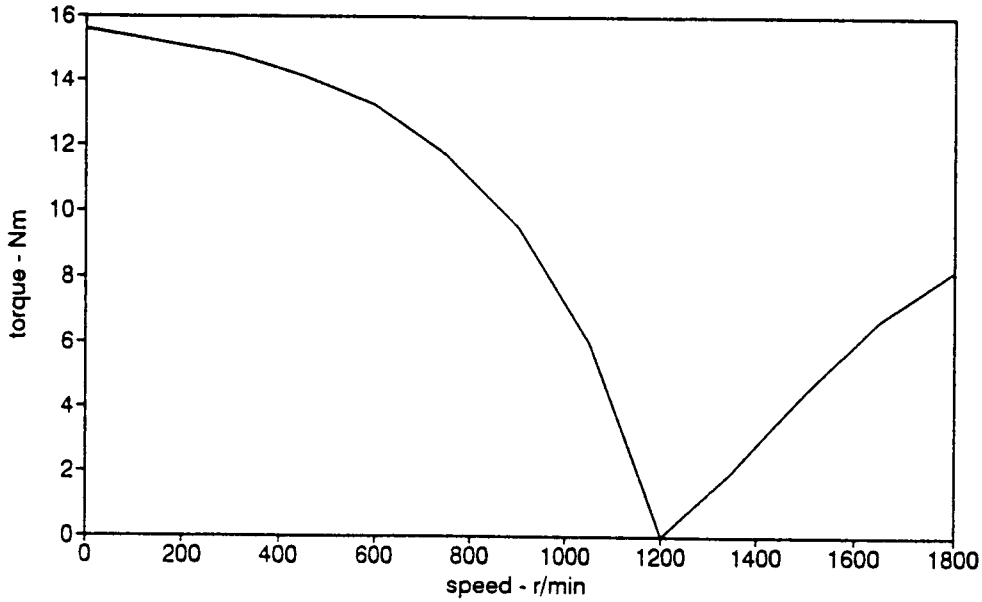


Figure 1.2: Torque-Limit Envelope of BDFM

(It should be noted that the BDFM under study has a higher torque-limit envelope than that shown in Figure 1.2; this is only a sample curve based on a test run of the machine at half of the rated 6-pole excitation.) Fourth, the BDFM exhibits poor open-loop dynamic response to step changes in speed command or load torque. This is illustrated in Figure 1.3.

Thus, the BDFM requires a feedback controller for dependable, high-performance operation, and this greatly increases the complexity and initial development cost of the system. Although the same is true for

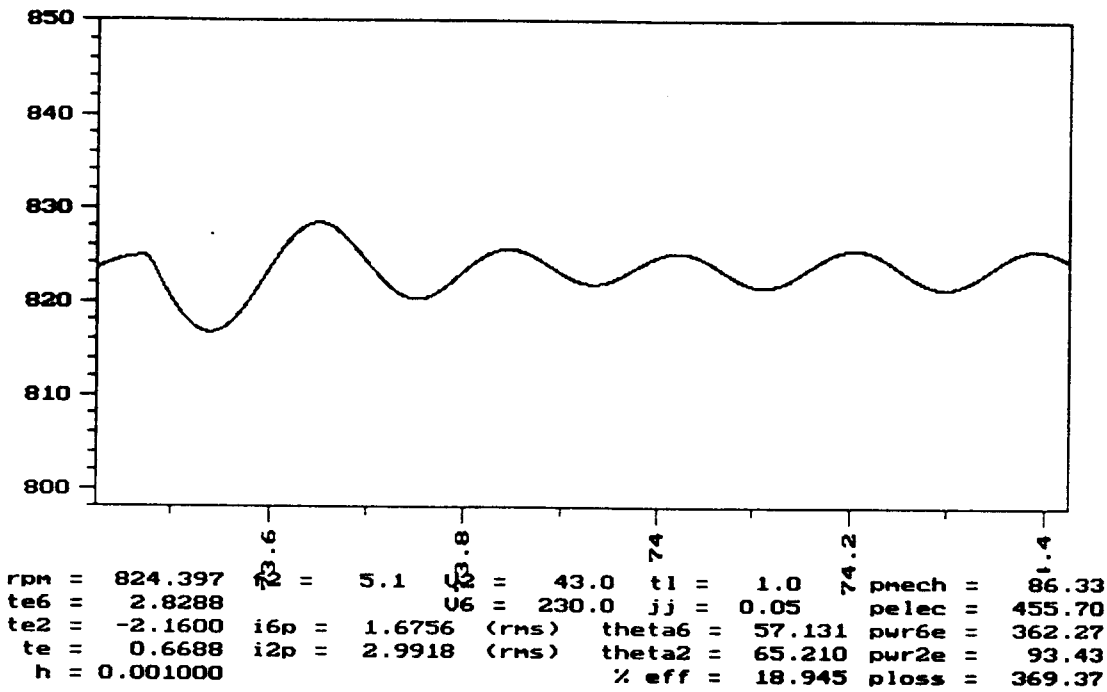


Figure 1.3: Undesirable Oscillatory Step Response of BDFM to Step Change in Load Torque (open-loop)

many conventional AC drives, the control problem at hand is unique due to the special nature of the BDFM. Third, the 6- and 2-pole BDFM is completely unable to support any load torque at exactly 1200 r/min, with or without a controller. Torque-producing capability steadily decreases as speed approaches 1200 r/min, either from above or from below. This is because the BDFM becomes the equivalent of two independent induction machines at this speed. The 6- and 2-pole magnetic fields, as well as the rotor, are all rotating at exactly the same speed at 1200 r/min, causing the rotor currents to go to zero. Consequently, no torque is produced at this speed. At this point, the only way to produce torque is to operate in the induction mode and use slip. The only way to produce slip is to deviate the rotor speed from 1200 r/min, which was the intended operating speed. The dynamics in this case are rather complex because the 6- and 2-pole systems again become coupled as soon as the slip is introduced, and the system exhibits a largely oscillatory response involving both synchronous and inductive operating modes, as illustrated in Figure 1.4. This phenomenon needs to be addressed by carefully selecting operating speed ranges and thus pole combinations for given applications.

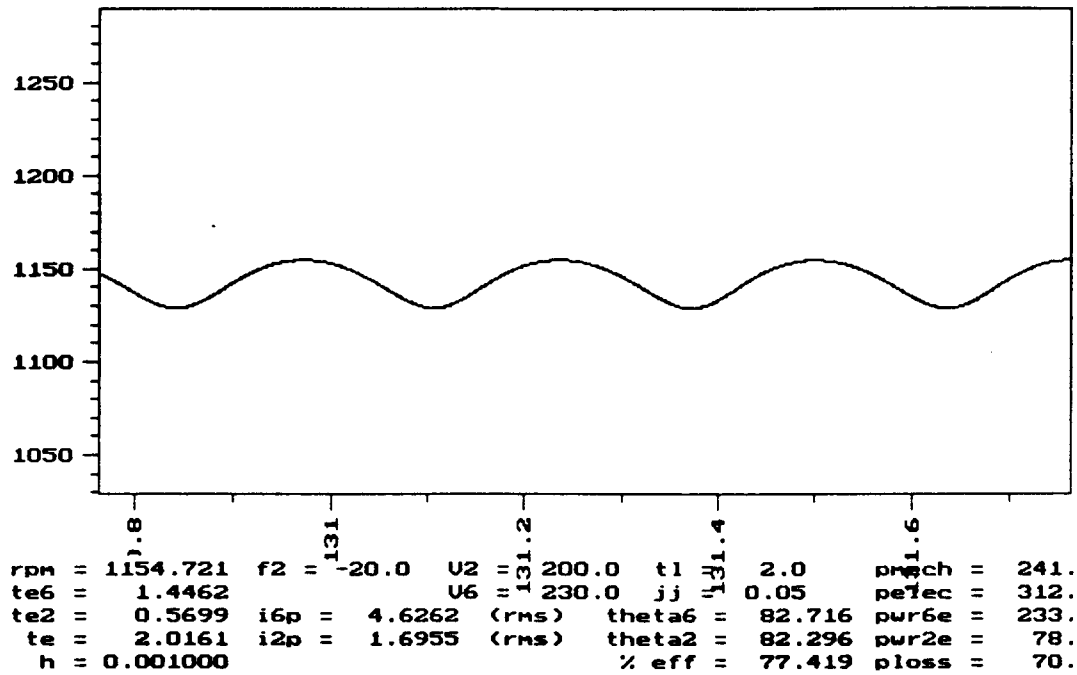


Figure 1.4: Oscillatory Response of BDFM near 1200 r/min

It should be noted that the BDFM is a very difficult machine to analyze mathematically. Its differential equations are nonlinear and time-varying, making controller development and stability analysis a considerable challenge. At speeds other than 1200 r/min, the 6-pole magnetic field, the 2-pole magnetic field, and the rotor are all turning at different speeds (and sometimes in different directions). As a result, there do not exist any reference frames in which all quantities are constants, making conventional analysis considerably more difficult than for conventional IM drives. (See [4].)

## 1.3 Control Considerations

Previous work [4] has illustrated control algorithms based on constant V/Hz schemes known from conventional induction motor drives. However, while this strategy assures open-loop stable operation of the doubly-fed drive, the dynamic response is poor and steady-state

performance is at times far from optimum. This motivates the development of a closed-loop torque and flux control scheme in order to achieve competitive drive performance.

Traditional methods of torque control in induction machines (IM) utilize a controlled current source and field orientation principles to determine the appropriate stator current reference which achieves torque and flux control. This type of control is not readily adaptable to the BDFM since the six-pole voltages and currents are not directly controllable. Alternatively, sliding mode schemes such as Direct Self Control [5,6] as well as those presented in [7,8] determine the inverter switching state directly from the torque and flux error; that is, without an inner current regulation loop. Existing sliding mode schemes are typically based on the fact that each of the inverter voltage vectors is known without calculation or knowledge of machine parameters to increase or decrease the torque and flux. Therefore, a hysteresis, or sliding mode control based on the torque and flux error can be easily formulated.

The direct formulation of a sliding surface to determine the inverter state, based only on the torque and flux error, is not available in the BDFM since the voltage vectors which drive the torque and flux in the correct direction are not explicitly known (nor can they be predicted) without calculating the actual torque and flux which results from a particular inverter voltage vector. This is due to the fact that the torque and flux depend on both controlled (two-pole) and uncontrolled (six-pole) quantities. Therefore, a predictive method which calculates an estimate of the change in flux and torque for a given set of inputs is appropriate. One such predictive, direct torque control scheme was presented in [9], for control of a squirrel cage IM. In the steady-state, this scheme calculates the value of stator voltage which results in the desired change in torque and flux.

In this thesis, a similar approach is used, as outlined in [10]. With the doubly-fed machine, the two-pole voltage is calculated which results in the desired changes in torque and flux. The predictive calculations use measured terminal quantities, rotor speed and position, and machine parameters. Space vector PWM can be used to determine the inverter switching function, resulting in a constant switching frequency. Alternatively, a resonant converter in the voltage mode can be appropriately controlled. Control update or switching frequency is kept at 1 kHz to ensure feasibility of real time implementation using a Digital Signal Processing (DSP) System.

## 1.4 Industrial Application Potential of BDFM

The BDFM has numerous possibilities in industry for improving efficiency and reducing costs. Paper mills rely on variable speed drives for turning the paper reels at a fairly constant linear speed so that a constant tension is maintained in the paper. The reels must turn quickly when nearly empty and more slowly when nearly full. Chemical processing plants use fans and fluid pumps to regulate temperatures and reaction rates. Sometimes this is achieved with fixed-speed pumps and the use of throttling, but this is inefficient; a better way to achieve variable fluid/air flow is to use a variable-speed pump, driven by a BDFM, without throttling. As mentioned earlier, maintenance is less frequent with the BDFM than it is with brush-type machines, making it useful for windmill generators and submersible pumps. Also, in applications where sparking in the motor could be hazardous in the presence of flammables, the BDFM has the advantage because it has no rubbing or intermittent electrical connections. The BDFM also shows promise in the area of automotive alternators; the typical "claw-rotor" type alternators in use today are at best 50% efficient, and with greater electrical demands expected on automobiles in the future, alternators will have to be made more efficient. The BDFM has the ability to regulate the output (battery-

charging) voltage with excitation level, while excitation frequency is a free variable which can be used to optimize efficiency. It has been shown in [11] that automotive alternators based on BDFMs can dramatically improve efficiency while maintaining a reasonable cost.

## 1.5 System Differential Equations for BDFM

The BDFM differential equations will not be derived entirely from basics here, for it is not the purpose of this thesis. (To see a complete derivation, see [12].) A brief summary of the equations, however, will be presented here, along with the specific machine paramaters used in this study.

Figure 1.5 shows the two-axis equivalent circuit for the BDFM, in the rotor reference frame. The zero-component is not shown because balanced three-phase is assumed. The system differential equations, shown in matrix form, are equivalent to Figure 1.5.

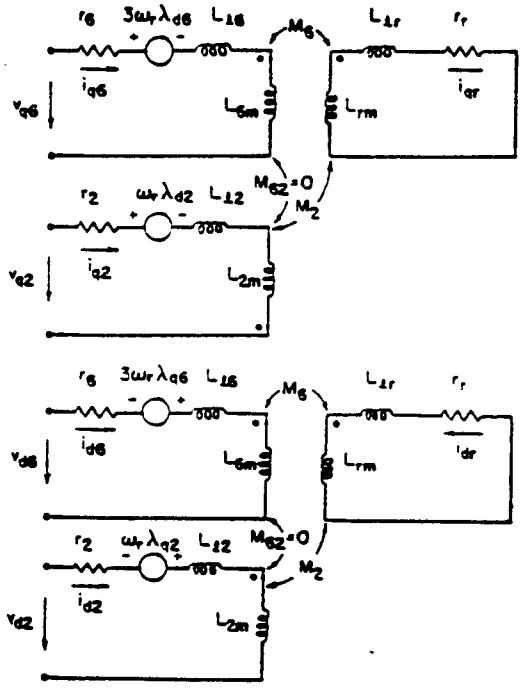


Figure 1.5: Two-Axis Equivalent Circuit

As derived in [13], the machine equations in the rotor reference frame are as follows:

$$\begin{bmatrix} v_{q6} \\ v_{d6} \\ v_{q2} \\ v_{d2} \\ v_{qr} \\ v_{dr} \end{bmatrix} = \begin{bmatrix} r_6+L_{s6}p & 3L_{s6}\omega_r & 0 & 0 & M_6p & 3M_6\omega_r \\ -3L_{s6}\omega_r & r_6+L_{s6}p & 0 & 0 & -3M_6\omega_r & M_6p \\ 0 & 0 & r_2+L_{s2}p & L_{s2}\omega_r & -M_2p & M_2\omega_r \\ 0 & 0 & -L_{s2}\omega_r & r_2+L_{s2}p & M_2\omega_r & M_2p \\ M_6p & 0 & -M_2p & 0 & r_r+L_rp & 0 \\ 0 & M_6p & 0 & M_2p & 0 & r_r+L_rp \end{bmatrix} \begin{bmatrix} i_{q6} \\ i_{d6} \\ i_{q2} \\ i_{d2} \\ i_{qr} \\ i_{dr} \end{bmatrix} \tag{1.3}$$

These machine equations, with some re-arranging and with the addition of the mechanical dynamics of the machine, are equivalent to the following:

System Differential Equations (8th-order):

$$di_{q6}/dt = \omega_r(3L_{1,1}AA_{1,8}+L_{1,4}AA_{4,8})i_{dr} + \omega_r(3A_{1,2}i_{d6}+A_{1,5}i_{d2}) - L_{1,1}v_{q6} + A_{1,1}i_{q6} + A_{1,4}i_{q2} + A_{1,7}i_{qr} - L_{1,4}v_{q2} \tag{1.4}$$

$$di_{d6}/dt = -\omega_r(3L_{2,2}AA_{2,7}+L_{2,5}AA_{5,7})i_{qr} - \omega_r(3A_{2,1}i_{q6}+A_{2,4}i_{q2}) + L_{2,2}v_{d6} + A_{2,2}i_{d6} + A_{2,5}i_{d2} + A_{2,8}i_{dr} - L_{2,5}v_{d2} \tag{1.5}$$

$$di_{q2}/dt = \omega_r(3L_{4,1}AA_{1,8}+L_{4,4}AA_{4,8})i_{dr} + \omega_r(3A_{4,2}i_{d6}+A_{4,5}i_{d2}) - L_{4,4}v_{q2} + A_{4,1}i_{q6} + A_{4,4}i_{q2} + A_{4,7}i_{qr} - L_{4,1}v_{q6} \tag{1.6}$$

$$di_{d2}/dt = -\omega_r(3L_{5,2}AA_{2,7}+L_{5,5}AA_{5,7})i_{qr} - \omega_r(3A_{5,1}i_{q6}+A_{5,4}i_{q2}) + L_{5,5}v_{d2} + A_{5,2}i_{d6} + A_{5,5}i_{d2} + A_{5,8}i_{dr} - L_{5,2}v_{d6} \tag{1.7}$$

$$di_{qr}/dt = \omega_r(3L_{7,1}AA_{1,8}+L_{7,4}AA_{4,8})i_{dr} + \omega_r(3A_{7,2}i_{d6}+A_{7,5}i_{d2}) - L_{7,1}v_{q6} + A_{7,1}i_{q6} + A_{7,4}i_{q2} + A_{7,7}i_{qr} - L_{7,4}v_{q2} \tag{1.8}$$

$$di_{dr}/dt = -\omega_r(3L_{8,2}AA_{2,7}+L_{8,5}AA_{5,7})i_{qr} - \omega_r(3A_{8,1}i_{q6}+A_{8,4}i_{q2}) + L_{8,2}v_{d6} + A_{8,2}i_{d6} + A_{8,5}i_{d2} + A_{8,8}i_{dr} - L_{8,5}v_{d2} \tag{1.9}$$

$$d\theta_r/dt = \omega_r \tag{1.10}$$

$$d\omega_r/dt = (t_e - t_l)/J \tag{1.11}$$

(See Appendix D for the definitions of the matrices A, AA, and L.)

The first six equations are equivalent to the two-axis equivalent circuit, while the last two equations represent the mechanical system of the machine.

The flux-current relationships in the machine may be expressed in the following form:

$$\begin{bmatrix} \lambda_{q6} \\ \lambda_{d6} \\ \lambda_{q2} \\ \lambda_{d2} \end{bmatrix} = \begin{bmatrix} L_{s6} & 0 & 0 & 0 & M_6 & 0 \\ 0 & L_{s6} & 0 & 0 & 0 & M_6 \\ 0 & 0 & L_{s2} & 0 & -M_2 & 0 \\ 0 & 0 & 0 & L_{s2} & 0 & M_2 \end{bmatrix} \begin{bmatrix} i_{q6} \\ i_{d6} \\ i_{q2} \\ i_{d2} \\ i_{qr} \\ i_{dr} \end{bmatrix} \qquad (1.12)$$

## 1.6 BDFM Literature

The following references are recommended for further understanding of the BDFM and the control methods which may be applied to it.


B.K. Bose, 'Power Electronics and AC Drives', Prentice-Hall, NJ, 1989.

R.A. DeCarlo, S.H. Zak, and G.P. Matthews, "Variable Structure Control of Nonlinear Multivariable Systems: A Tuturial", IEEE Proceedings, vol. 76, no. 3, pp. 212-232, 1988.

P.C. Krause, 'Analysis of Electric Machinery', McGraw-Hill, NY, 1986.

R. Li, A. Wallace, and R. Spee, "Dynamic Simulation of Brushless Doubly-Fed Machines", IEEE Trans. Energy Conv., vol 6, no. 3, pp. 445-452, 1991.

R. Li, A. Wallace, R. Spee, and Y. Wang, "Two-Axis Model of Cage-Rotor Brushless Doubly-Fed Machines", IEEE Trans. Energy Conv., vol 6, no. 3, pp. 453-460, 1991.

R.D. Lorenz and D.B. Lawson, "A Simplified Approach to Continuous On-Line Tuning of Field-Oriented Induction Machine Drives", IEEE Trans. IAS, vol. 26, no. 3, pp. 420-424, 1990.

P.K. Nandam and P.C. Sen, "Sliding Mode Speed Control of a Self Controlled Synchronous Motor (SCSM) Using and Adaptive State Observer", Third Int'l Conference on Power Electronics and Variable Speed Drives, IEE Conference Publication, no. 291, pp. 315-318, 1988.

R. Spee, A.K. Wallace, and H.K. Lauw, "Performance Simulation of Brushless Doubly-Fed Adjustable Speed Drives", IEEE-IAS Annual Meeting Conference Record, pp. 738-743, 1989.

J. Zhang and T.H. Barton, "A Fast Variable Structure Current Controller for an Induction Machine Drive", IEEE Trans. IAS, vol. 26, no. 3, pp. 415-419, 1990.

# Chapter 2

# Controller Development for BDFM

## 2.1 Statement of Control Problem

The quantity to be controlled is the rotor (shaft) speed of the BDFM. For a commanded speed given by the user of the system, the controller must be able to do the following: regulate the shaft speed to the commanded value, while compensating for variations in load torque and 6-pole voltage; be able to quickly and accurately track changes in the command speed, with minimal rise time and overshoot for an input step change; be able to stabilize torque/speed regions which are open-loop unstable and expand the torque/speed capabilities of the BDFM. In addition to these requirements, the controller should have a slower, outer loop which seeks the 2-pole flux (excitation) level which produces the optimum combination of efficiency and power factor for the system.

Once the controller requirements have been defined, the controller design constraints can be formalized: The controller must satisfy the above requirements by controlling only two parameters: the q and d components of the 2-pole voltage ($v_{q2}$ and $v_{d2}$). These are the only two system inputs which may be freely changed; the 6-pole inputs are fixed to the power grid. Equivalently, only the magnitude and frequency of the 2-pole input voltage may be used to control the machine.

## 2.2 Selection of Control Strategy

The first step in the controller design, as described in section 1.3, is the investigation of traditional control strategies. Stator current control, based on field-orientation principles, is not possible because only the 2-pole current can be directly controlled. Sliding mode torque

control, while attractive in terms of robustness, is not feasible for the BDFM because the existence conditions are too difficult to solve analytically; the equations for the existence conditions are 6-dimensional, coupled, and nonlinear. Traditional vector control also isn't possible, because there does not exist any reference frame in which all quantities are constant.

Predictive direct torque control is the method ultimately chosen for the task. Ref. [9] presents the successful application of direct torque control to a singly-fed induction motor drive, with a space-vector pulse width modulation (PWM) converter; this method of control can be generalized to include doubly-fed machines. The mathematics of the controller design, in both cases, is quite similar in method and structure. In both systems, a digital signal processing (DSP) system is used for real-time control.

## 2.3 Development of Direct Torque Control Algorithm

The most important equation in the development of direct torque control is the torque equation and its derivative. The torque equation, like that of a singly-fed machine, can be expressed as the cross-product of stator and rotor currents, multiplied by mutual inductances. (See Appendix B for a glossary of terms.)

$$\tau_{e6} = 3M_6(i_{q6}i_{dr} - i_{d6}i_{qr}) = \text{6-pole torque component} \quad (2.1)$$

$$\tau_{e2} = M_2(i_{q2}i_{d6} + i_{d2}i_{qr}) = \text{2-pole torque component} \quad (2.2)$$

$$\tau_e = \tau_{e6} + \tau_{e2} = 3M_6(i_{q6}i_{dr} - i_{d6}i_{qr}) + M_2(i_{q2}i_{d6} + i_{d2}i_{qr}) \quad (2.3)$$
$$= \text{total electrical torque}$$

These equations are easily expressed in terms of stator quantities, by substituting the appropriate expressions for the rotor currents:

$$\tau_{e6} = 3[i_{q6}(\lambda_{d6} - L_{s6}i_{d6}) - i_{d6}(\lambda_{q6}-L_{s6}i_{q6})] \quad (2.4)$$
$$= 3(i_{q6}\lambda_{d6} - i_{d6}\lambda_{q6})$$
$$\tau_{e2} = i_{q2}(\lambda_{d2} - L_{s2}i_{d2}) + i_{d2}(L_{s2}i_{q2} - \lambda_{q2}) \quad (2.5)$$
$$= (i_{q2}\lambda_{d2} - i_{d2}\lambda_{q2})$$

$$\tau_e = \tau_{e6} + \tau_{e2} = 3(i_{q6}\lambda_{d6} - i_{d6}\lambda_{q6}) + (i_{q2}\lambda_{d2} - i_{d2}\lambda_{q2}) \quad (2.6)$$

This yields the torque equation expressed as the cross products of stator currents and fluxes, with a derivative of

$$\dot{\tau}_{e6} = 3(i_{q6}\dot{\lambda}_{d6}+\dot{i}_{q6}\lambda_{d6}-i_{d6}\dot{\lambda}_{q6}-\dot{i}_{d6}\lambda_{q6}) \quad (2.7)$$
$$\dot{\tau}_{e2} = (i_{q2}\dot{\lambda}_{d2}+\dot{i}_{q2}\lambda_{d2}-i_{d2}\dot{\lambda}_{q2}-\dot{i}_{d2}\lambda_{q2}) \quad (2.8)$$

$$\dot{\tau}_e = \dot{\tau}_{e6} + \dot{\tau}_{e2} \quad (2.9)$$
$$= 3(i_{q6}\dot{\lambda}_{d6}+\dot{i}_{q6}\lambda_{d6}-i_{d6}\dot{\lambda}_{q6}-\dot{i}_{d6}\lambda_{q6}) + (i_{q2}\dot{\lambda}_{d2}+\dot{i}_{q2}\lambda_{d2}-i_{d2}\dot{\lambda}_{q2}-\dot{i}_{d2}\lambda_{q2})$$

For the controller design, the goal is to find the values of $v_{q2}$ and $v_{d2}$ which will yield a desired value of $\dot{\tau}_e$. By controlling this quantity, the torque itself may be controlled. (This is discussed later.) In order to solve for $v_{q2}$ and $v_{d2}$, $\dot{\tau}_e$ must be expressed entirely in terms of known quantities and in terms of the two unknowns to be solved for. (As discussed later, a second equation is required to ensure a unique solution.)

A few of the terms in 2.9 are easy to obtain. The stator currents iq6, iq2, id6, and id2 are directly measured in the abc-domain with current transducers and are simply transformed to the rotor qd0 reference frame, using the angular position ($\theta_r$) of the rotor.

$$\begin{bmatrix} i_{q6} \\ i_{d6} \\ i_{06} \end{bmatrix} = \text{sqrt}(2/3) \begin{bmatrix} \cos(3\theta_r) & \cos(3\theta_r-2\pi/3) & \cos(3\theta_r+2\pi/3) \\ \sin(3\theta_r) & \sin(3\theta_r-2\pi/3) & \sin(3\theta_r+2\pi/3) \\ 1 & 1 & 1 \end{bmatrix} \begin{bmatrix} i_{a6} \\ i_{b6} \\ i_{c6} \end{bmatrix} \quad (2.10)$$

$$\begin{bmatrix} i_{q2} \\ i_{d2} \\ i_{02} \end{bmatrix} = \text{sqrt}(2/3) \begin{bmatrix} \cos(\theta_r - 2\pi/9) & \cos(\theta_r - 2\pi/9 - 2\pi/3) & \cos(\theta_r - 2\pi/9 + 2\pi/3) \\ \sin(\theta_r - 2\pi/9) & \sin(\theta_r - 2\pi/9 - 2\pi/3) & \sin(\theta_r - 2\pi/9 + 2\pi/3) \\ 1 & 1 & 1 \end{bmatrix} \begin{bmatrix} i_{a2} \\ i_{b2} \\ i_{c2} \end{bmatrix} \tag{2.11}$$

The fluxes are more difficult to obtain. In order to save on system cost, it is desirable to avoid Hall-effect transducers in the machine. Thus, fluxes are estimated from terminal quantities, by integrating the terminal voltages of the machine, compensating for the I-R drops. The flux derivatives in the rotor reference frame are the following:

$$\dot{\lambda}_{q6r} = v_{q6r} - i_{q6r}r_6 - 3\omega_r\lambda_{d6r} \tag{2.12}$$

$$\dot{\lambda}_{d6r} = v_{d6r} - i_{d6r}r_6 + 3\omega_r\lambda_{q6r} \tag{2.13}$$

$$\dot{\lambda}_{q2r} = v_{q2r} - i_{q2r}r_6 - \omega_r\lambda_{d2r} \tag{2.14}$$

$$\dot{\lambda}_{d2r} = v_{d2r} - i_{d2r}r_6 + \omega_r\lambda_{q2r} \tag{2.15}$$

To find the rotor reference frame fluxes, it would intuitively make sense to directly integrate the derivatives of these fluxes, in the rotor reference frame. Unfortunately, this causes a problem. As illustrated in 2.12 through 2.15, the flux derivatives contain speed-voltage terms, which couple the equations into pairs and make integration difficult. This problem is easily avoided, however, by integrating the flux derivatives in the stationary reference frame. This decouples the differential equations, so that they may be integrated separately.

$$\dot{\lambda}_{q6s} = v_{q6s} - i_{q6s}r_6 \tag{2.16}$$

$$\dot{\lambda}_{d6s} = v_{d6s} - i_{d6s}r_6 \tag{2.17}$$

$$\dot{\lambda}_{q2s} = v_{q2s} - i_{q2s}r_6 \tag{2.18}$$

$$\dot{\lambda}_{d2s} = v_{d2s} - i_{d2s}r_6 \tag{2.19}$$

$$\lambda_{q6s} = \int_0^t (v_{q6s} - i_{q6s}r_6)d\tau \tag{2.20}$$

$$\lambda_{d6s} = \int_0^t (v_{d6s} - i_{d6s}r_6)d\tau \tag{2.21}$$

$$\lambda_{q2s} = \int_0^t (v_{q2s} - i_{q2s}r_2)d\tau \tag{2.22}$$

$$\lambda_{d2s} = \int_0^t (v_{d2s} - i_{d2s}r_2)d\tau \tag{2.23}$$

These expressions are then transformed to the rotor reference frame:

$$\begin{bmatrix} \lambda_{q6r} \\ \lambda_{d6r} \end{bmatrix} = \begin{bmatrix} \cos(3\theta_r) & -\sin(3\theta_r) \\ \sin(3\theta_r) & \cos(3\theta_r) \end{bmatrix} \begin{bmatrix} \lambda_{q6s} \\ \lambda_{d6s} \end{bmatrix} \tag{2.24}$$

$$\begin{bmatrix} \lambda_{q2r} \\ \lambda_{d2r} \end{bmatrix} = \begin{bmatrix} \cos(\theta_r - 2\pi/9) & -\sin(\theta_r - 2\pi/9) \\ \sin(\theta_r - 2\pi/9) & \cos(\theta_r - 2\pi/9) \end{bmatrix} \begin{bmatrix} \lambda_{q2s} \\ \lambda_{d2s} \end{bmatrix} \tag{2.25}$$

Other quantities which must be identified are $\dot{\lambda}_{q6}$, $\dot{\lambda}_{d6}$, $\dot{\lambda}_{q2}$, and $\dot{\lambda}_{d2}$. These are easily found from evaluating the flux differential equations shown above for the rotor reference frame (2.12 - 2.15). Note that $\dot{\lambda}_{q2}$ and $\dot{\lambda}_{d2}$ also depend on $v_{q2}$ and $v_{d2}$, the quantities to be solved for by the controller.

Finally, the remaining quantities to be solved for are the current derivatives, $\dot{i}_{q6}$, $\dot{i}_{d6}$, $\dot{i}_{q2}$, and $\dot{i}_{d2}$. These are the most difficult quantities to estimate and are a critical process step in the direct torque control of the machine. Efforts were made to estimate the current derivatives by extrapolating the currents with a steady-state approximation, as in [9]. As might be expected, this proved effective only in the steady-state; estimation accuracy under dynamic conditions was unacceptable. It was decided that the only way to obtain reliable current-derivative quantities was to evaluate the differential equations of the machine, in the rotor reference frame. This method of estimation has some serious drawbacks; it requires fairly accurate knowledge of all machine parameters, plus the knowledge of the instantaneous rotor currents, which can't be directly measured. Fortunately, if the stator currents and fluxes are known, then the rotor currents can be calculated, using the following equations:

$$i_{qr} = (\lambda_{q6} - L_{s6} i_{q6})/M_6 \tag{2.26}$$

$$i_{dr} = (\lambda_{d6} - L_{s6} i_{d6})/M_6 \tag{2.27}$$

Thus, the current derivative equations in the rotor reference frame can be written as follows: (see Appendix D for definitions of A and L matrices)

$$\dot{i}_{q6} = \omega_r(3L_{1,1}A_{1,8}+L_{1,4}A_{4,8})i_{dr} + \omega_r(3A_{1,2}i_{d6}+A_{1,5}i_{d2}) \quad (2.28)$$
$$- L_{1,1}v_{q6} + A_{1,1}i_{q6} + A_{1,4}i_{q2} + A_{1,7}i_{qr} - L_{1,4}v_{q2}$$

$$\dot{i}_{d6} = -\omega_r(3L_{2,2}A_{2,7}+L_{2,5}A_{5,7})i_{qr} - \omega_r(3A_{2,1}i_{q6}+A_{2,4}i_{q2}) \quad (2.29)$$
$$+ L_{2,2}v_{d6} + A_{2,2}i_{d6} + A_{2,5}i_{d2} + A_{2,8}i_{dr} - L_{2,5}v_{d2}$$

$$\dot{i}_{q2} = \omega_r(3L_{4,1}A_{1,8}+L_{4,4}A_{4,8})i_{dr} + \omega_r(3A_{4,2}i_{d6}+A_{4,5}i_{d2}) \quad (2.30)$$
$$- L_{4,4}v_{q2} + A_{4,1}i_{q6} + A_{4,4}i_{q2} + A_{4,7}i_{qr} - L_{4,1}v_{q6}$$

$$\dot{i}_{d2} = -\omega_r(3L_{5,2}A_{2,7}+L_{5,5}A_{5,7})i_{qr} - \omega_r(3A_{5,1}i_{q6}+A_{5,4}i_{q2}) \quad (2.31)$$
$$+ L_{5,5}v_{d2} + A_{5,2}i_{d6} + A_{5,5}i_{d2} + A_{5,8}i_{dr} - L_{5,2}v_{d6}$$

Thus, the current derivatives are expressed entirely in terms of known quantities and the control variables $v_{q2}$ and $v_{d2}$, which will be solved for.

At this point, it is convenient to introduce new variable definitions and substitutions to make the equations manageable.

Let $\dot{i}_{q6} = \alpha_1 - L_{1,4}v_{q2}$, where (2.32)

$$\alpha_1 = \omega_r(3L_{1,1}A_{1,8}+L_{1,4}A_{4,8})i_{dr} + \omega_r(3A_{1,2}i_{d6}+A_{1,5}i_{d2}) \quad (2.33)$$
$$- L_{1,1}v_{q6} + A_{1,1}i_{q6} + A_{1,4}i_{q2} + A_{1,7}i_{qr}$$

Let $\dot{i}_{d6} = \alpha_2 - L_{2,5}v_{d2}$, where (2.33)

$$\alpha_2 = -\omega_r(3L_{2,2}A_{2,7}+L_{2,5}A_{5,7})i_{qr} - \omega_r(3A_{2,1}i_{q6}+A_{2,4}i_{q2}) \quad (2.34)$$
$$+ L_{2,2}v_{d6} + A_{2,2}i_{d6} + A_{2,5}i_{d2} + A_{2,8}i_{dr}$$

Let $\dot{i}_{q2} = \alpha_3 - L_{4,4}v_{q2}$, where (2.35)

$$\alpha_3 = \omega_r(3L_{4,1}A_{1,8}+L_{4,4}A_{4,8})i_{dr} + \omega_r(3A_{4,2}i_{d6}+A_{4,5}i_{d2}) \quad (2.36)$$
$$+ A_{4,1}i_{q6} + A_{4,4}i_{q2} + A_{4,7}i_{qr} - L_{4,1}v_{q6}$$

Let $\dot{i}_{d2} = \alpha_4 - L_{5,5}v_{d2}$, where (2.37)

$$\alpha_4 = -\omega_r(3L_{5,2}A_{2,7}+L_{5,5}A_{5,7})i_{qr} - \omega_r(3A_{5,1}i_{q6}+A_{5,4}i_{q2}) \quad (2.38)$$
$$+ A_{5,2}i_{d6} + A_{5,5}i_{d2} + A_{5,8}i_{dr} - L_{5,2}v_{d6}$$

For the flux derivatives: (rotor reference frame)

Let $\dot{\lambda}_{q2} = v_{q2} - \alpha_5$, where (2.39)

$$\alpha_5 = i_{q2}r_6 + \omega_r\lambda_{d2} \quad (2.40)$$

Let $\dot{\lambda}_{d2} = v_{d2} - \alpha_6$, where (2.41)

$$\alpha_6 = i_{d2}r_6 + \omega_r\lambda_{q2} \quad (2.42)$$

With these substitutions, the torque command derivative equations become

$$\dot{t}^*_{e6} = 3(i_{q6}\dot{\lambda}_{d6}+\dot{i}_{q6}\lambda_{d6}-i_{d6}\dot{\lambda}_{q6}-\dot{i}_{d6}\lambda_{q6}) = \quad (2.43)$$
$$3[i_{q6}\dot{\lambda}_{d6} + (\alpha_1-L_{1,4}v_{q2})\lambda_{d6} - i_{d6}\dot{\lambda}_{q6} - (\alpha_2-L_{2,5}v_{d2})\lambda_{q6}]$$

$$\dot{t}^*_{e2} = i_{q2}\dot{\lambda}_{d2}+\dot{i}_{q2}\lambda_{d2}-i_{d2}\dot{\lambda}_{q2}-\dot{i}_{d2}\lambda_{q2} = \quad (2.44)$$
$$i_{q2}(v_{d2}-\alpha_6) + (\alpha_3-L_{4,4}v_{q2})\lambda_{d2} - i_{d2}(v_{q2}-\alpha_5) - (\alpha_4-L_{5,5}v_{d2})\lambda_{q2}$$

Combining these and collecting terms yields:

$$\dot{t}^*_e = \dot{t}^*_{e6} + \dot{t}^*_{e2}$$
$$= 3(i_{q6}\dot{\lambda}_{d6}+\dot{i}_{q6}\lambda_{d6}-i_{d6}\dot{\lambda}_{q6}-\dot{i}_{d6}\lambda_{q6}) + (i_{q2}\dot{\lambda}_{d2}+\dot{i}_{q2}\lambda_{d2}-i_{d2}\dot{\lambda}_{q2}-\dot{i}_{d2}\lambda_{q2})$$
$$= \beta_1 v_{q2} + \beta_2 v_{d2} + \beta_3, \text{ where} \quad (2.45)$$

$$\beta_1 = -3L_{1,4}\lambda_{d6} - L_{4,4}\lambda_{d2} - i_{d2} \quad (2.46)$$

$$\beta_2 = 3L_{2,5}\lambda_{q6} + i_{q2} + L_{5,5}\lambda_{q2} \quad (2.47)$$

$$\beta_3 = -i_{q2}\alpha_6 + \alpha_3\lambda_{d2} + i_{d2}\alpha_5 - \alpha_4\lambda_{q2} \quad (2.48)$$

At this point, the equations have been simplified to a single linear equation with two unknowns. It is thus necessary to define a constraining condition to create another equation, so that a unique solution may be found for $v_{q2}$ and $v_{d2}$. 2-pole flux level is the logical choice; it is directly controllable by the converter, and it represents the excitation level of the machine, as does the DC excitation in a singly-fed synchronous machine. Power factor and efficiency are strongly influenced by the 2-pole excitation level, and this fact will be used in a slower, outer control loop to optimize the steady-state performance of the machine.

The 2-pole flux level in the machine is expressed as

$$\lambda_2 = \text{sqrt}(\lambda^2_{q2} + \lambda^2_{d2}) \quad (2.49)$$

Squaring and taking the derivative yields

$$\lambda_{q2}\dot{\lambda}_{q2} + \lambda_{d2}\dot{\lambda}_{d2} = \lambda_2\dot{\lambda}_2 = \dot{\lambda}_2\text{sqrt}(\lambda_{q2}^2+\lambda_{d2}^2) \tag{2.50}$$

After substituting equations 2.39 and 2.41 for $\dot{\lambda}_{q2}$ and $\dot{\lambda}_{d2}$, this becomes

$$\lambda_{q2}(v_{q2}-\alpha_5)/\text{sqrt}(\lambda_{q2}^2+\lambda_{d2}^2) + \lambda_{d2}(v_{d2}-\alpha_6)/\text{sqrt}(\lambda_{q2}^2+\lambda_{d2}^2) = \dot{\lambda}_2 \tag{2.51}$$

Collecting terms and simplifying yields a second linear equation for $v_{q2}$ and $v_{d2}$, for a given flux command:

$$\beta_4 v_{q2} + \beta_5 v_{d2} + \beta_6 = \dot{\lambda}_2^*, \text{ where} \tag{2.52}$$

$$\beta_4 = \lambda_{q2}/\text{sqrt}(\lambda_{q2}^2+\lambda_{d2}^2) \tag{2.53}$$

$$\beta_5 = \lambda_{d2}/\text{sqrt}(\lambda_{q2}^2+\lambda_{d2}^2) \tag{2.54}$$

$$\beta_6 = -(\lambda_{q2}\alpha_5+\lambda_{d2}\alpha_6)/\text{sqrt}(\lambda_{q2}^2+\lambda_{d2}^2) \tag{2.55}$$

Thus, equations 2.45 and 2.52 represent 2 linear equations and 2 unknowns; summarizing this yields

$$\begin{bmatrix} \beta_1 & \beta_2 \\ \beta_4 & \beta_5 \end{bmatrix} \begin{bmatrix} v_{q2} \\ v_{d2} \end{bmatrix} = \begin{bmatrix} \dot{t}_e^*-\beta_3 \\ \dot{\lambda}_2^*-\beta_6 \end{bmatrix} \tag{2.56}$$

Solving 2.56 gives

$$\begin{bmatrix} v_{q2} \\ v_{d2} \end{bmatrix} = \frac{1}{\beta_1\beta_5-\beta_2\beta_4} \begin{bmatrix} \beta_5 & -\beta_2 \\ -\beta_4 & \beta_1 \end{bmatrix} \begin{bmatrix} \dot{t}_e^*-\beta_3 \\ \dot{\lambda}_2^*-\beta_6 \end{bmatrix} \tag{2.57}$$

This will always yield a unique solution for $v_{q2}$ and $v_{d2}$, as long as the "beta" matrix is nonsingular. (An error trap dealing with matrix singularities is required to solve for a converter output which will maximize the torque derivative and try to force the system back into synchronous operation as quickly as possible.)

Since $\dot{t}_e$ and $\dot{\lambda}_2$ can be directly controlled, a deadbeat type of controller can theoretically be used for torque and flux control of the BDFM, using the "direct torque control" scheme shown above as the innermost loop. Deadbeat

control isn't the only choice, however; a wide variety of control schemes may also be applied, such as sliding-mode or linear control. (If linear control is used, it should be adaptive and use some form of on-line parameter estimation.)

At this time, a simple linear PI controller is being implemented around the Direct Torque Control scheme. It is non-adaptive in nature and has been designed to test the validity of the Direct Torque Control equations and method in general. Figure 2.1 shows a block diagram of the resulting controller.

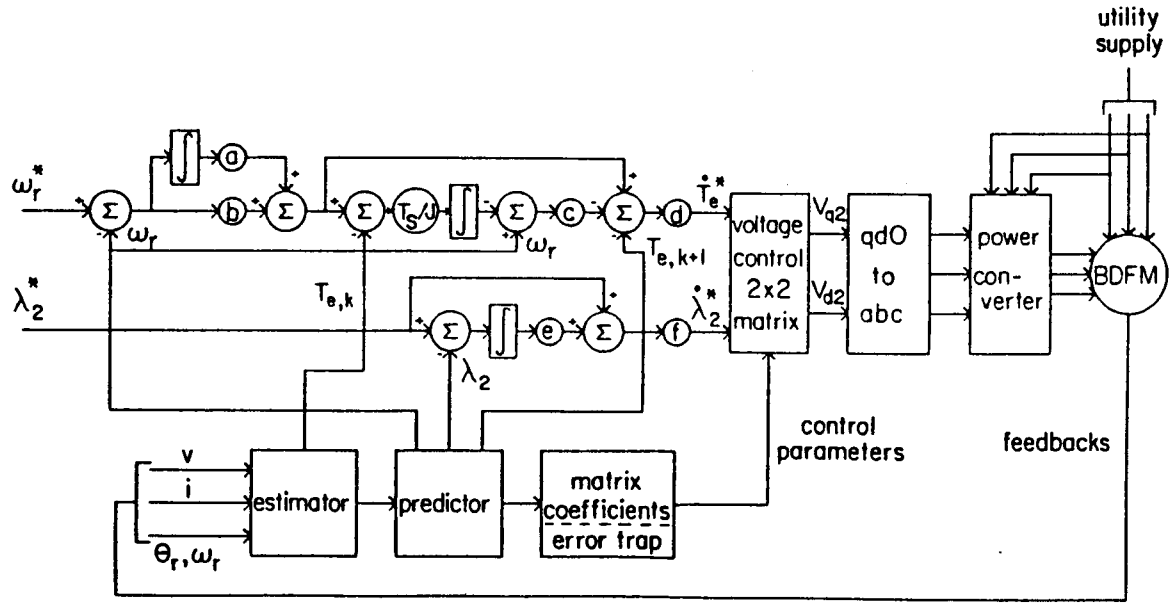


Figure 2.1: BDFM Controller Block Diagram

There are two inputs to the system; $\omega_r^*$ (the desired speed), and $\lambda_2^*$ (the desired 2-pole flux level). $\omega_r^*$ is specified directly by the user of the machine, or by an outer control loop in a position-servo system. $\lambda_2^*$ is specified directly or possibly by a slower, outer search loop which optimizes efficiency or power factor.

As shown in Fig 2.1, signals from the transducers (voltage, current, position, speed) are fed into the state estimator. Here, all voltages,

currents, and fluxes are calculated in the rotor reference frame. The next block, the predictor, estimates the state of the system after one controller update period; this compensates for computation lag. In the next block, the torque and flux equations are used, along with the flux and current derivatives, to determine the matrix coefficients. Here, the matrix is tested for singularity, and the error trap is used if necessary.

If the control matrix is nonsingular, torque and flux derivative commands are fed into the matrix equation to determine the excitation for the next controller period. This is converted back to abc-coordinates and fed into the power converter.

Torque and flux derivative commands are determined by a simple PI regulator, as shown in Fig 2.1. The speed loop has two integrators to eliminate steady-state error in the torque and speed, respectively. An additional integrator eliminates steady-state flux error. The stability and response of the PI loops is adjusted with the 6 gains, a-f. It should be noted again that PI control is just one of many control schemes that could be used here. Deadbeat or sliding mode control could also have been used. The Direct Torque Control algorithm, however, would always be in effect, as it is centered around the voltage control matrix.

The Direct Torque Control scheme designed in this thesis is intended to operate in the discrete-time domain, using a DSP. The calculations outlined above are quite lengthy, and a sampling period of 1 ms has been chosen to allow the DSP enough time to perform them. Unfortunately, the control voltages $v_{q2}$ and $v_{d2}$ which are calculated are the correct values to apply to the machine at the time of data sampling. By the time the next A/D and D/A strobe signal arrives, these control voltages are one controller update period too late. The predictor block has been included in the design of the controller to compensate for this delay, by predicting the state of the machine one sampling period after the data is sampled. This is a very

simple, straightforward process; the system differential equations (in the rotor reference frame) are simply evaluated, and the state variables are integrated one sampling period into the future. The differential equations used in the predictor are as shown in the introduction and need not be repeated here.

## 2.4 Outer Control Loop Development

The details of the outer (flux) control loop are not the subject of this thesis. The primary responsibility of this loop is to maintain a flux level in the machine which provides the necessary dynamic stability. Too much 2-pole flux, or too little, will cause the machine to stall or oscillate in a complex combination of 6-pole and 2-pole induction modes. Such behavior is prevented by carefully monitoring the determinant of the voltage control matrix (the "beta" matrix in equation 2.56). If the determinant of this matrix starts to approach zero, then controller failure becomes likely. In general, higher load torques require higher 2-pole flux levels to maintain stability; at higher speeds, the machine generally requires less 2-pole flux for a given load torque. Perhaps a better way for the controller to monitor system stability is to look at the "normalized" determinant of the control matrix, rather than the "absolute" determinant. This is because an ill-conditioned matrix (with significant skew from the orthogonal) can still have a large determinant, if the matrix elements are large enough. Normalizing the determinant would reveal the angle between the rows of the matrix, and the controller would select a flux level to maintain orthogonality.

The other responsibility of this outer loop is to optimize steady-state performance by appropriate selection of the 2-pole flux level (excitation). A search loop would attempt to maximize some quantity such as (power factor)*(efficiency). Interestingly, and fortunately, the flux levels which achieve this are generally very close to the flux levels which optimize dynamic stability and performance, as observed in numerous closed-loop simulations.

# Chapter 3

## Simulations and Evaluation of Controller Performance

### 3.1 Open vs. Closed Loop Step Responses

Using the "BDFMC41Y.PAS" revision of the BDFM/Controller Simulator written in Turbo Pascal 6.0 (see Appendix J), the drive was simulated in both open-and closed-loop operating modes and subjected to step changes in load torque and command speed. In all tests, the BDFM was first set up to operate in the steady-state, with a 7.5 Nm load torque. 2-pole flux level was chosen for maximum efficiency of operation and was maintained at this level during the transient. Two sets of data were taken; one set at 600 r/min, and the other at 1500 r/min. These two speeds were chosen for simulation for the following reasons:

1) Both sides of 1200 r/min speed barrier are represented.
2) Both abc and acb excitations are represented in the 2-pole.
3) Both speeds are capable of supporting reasonable load torques.

Figures 3.1a and 3.1b illustrate the differences between the open- and closed-loop responses, in shaft speed, to a -1 Nm step change in load torque, at 600 r/min. It is readily apparent that the closed-loop response settles much faster than the open-loop response and is less oscillatory in nature. In the open loop, the speed increases by roughly 8 r/min and then oscillates for about 1 second before settling appreciably. In the closed loop, the speed increases by only 0.7 r/min and settles in 50 ms, with far less oscillation. Clearly, the closed-loop speed regulation is superior to that of the open-loop.

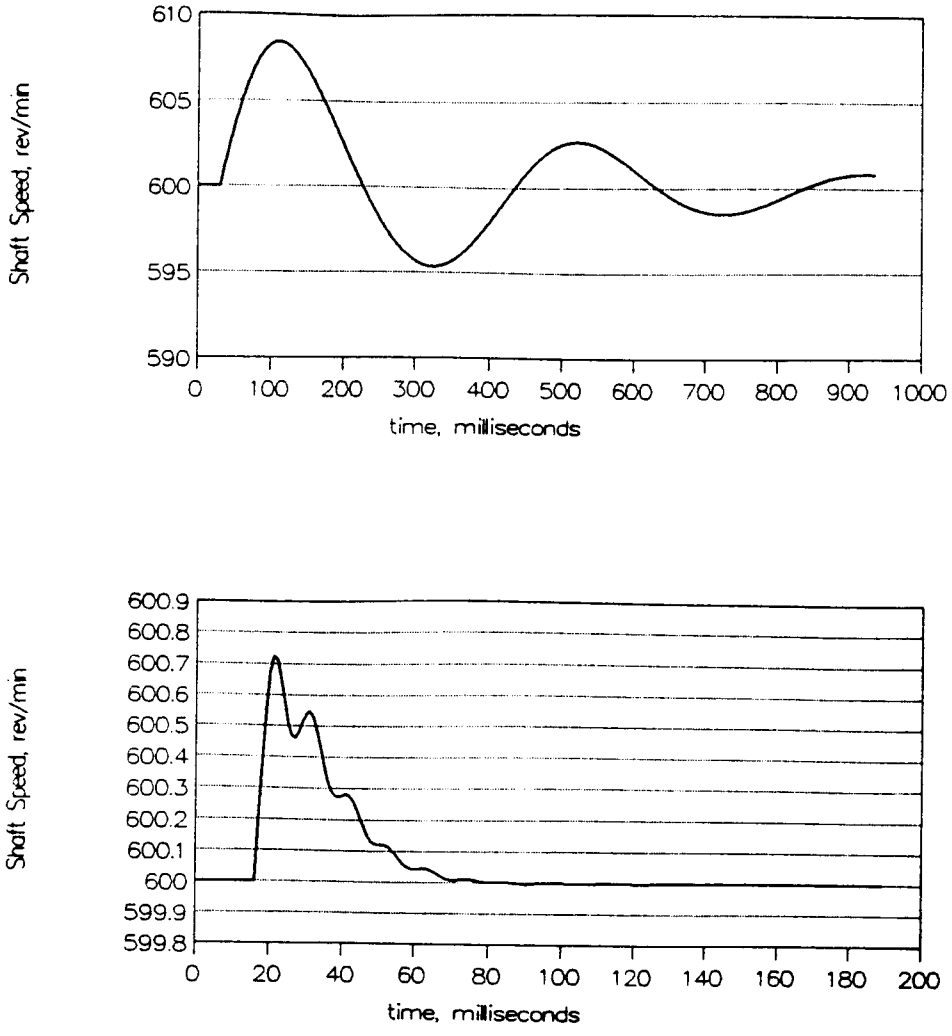


Figure 3.1: Response to Load Torque Disturbance (1 Nm step decrease at 600 r/min); Shaft Speed
a) open-loop; b) closed-loop

Figures 3.2a and 3.2b illustrate the differences between the open- and closed-loop responses, in 2-pole flux level, to the -1 Nm step change in load torque, at 600 r/min. Again, it is readily apparent that the open- and closed-loop responses differ considerably. In the open loop, the 2-pole flux level has a high frequency oscillation (of the electrical sub-system) superimposed over a low frequency oscillation (of the mechanical sub-system); these last significantly longer than one second. In the closed

loop, the peak-to-peak magnitude of the oscillation is roughly the same, but it decays to zero after about 50 ms.

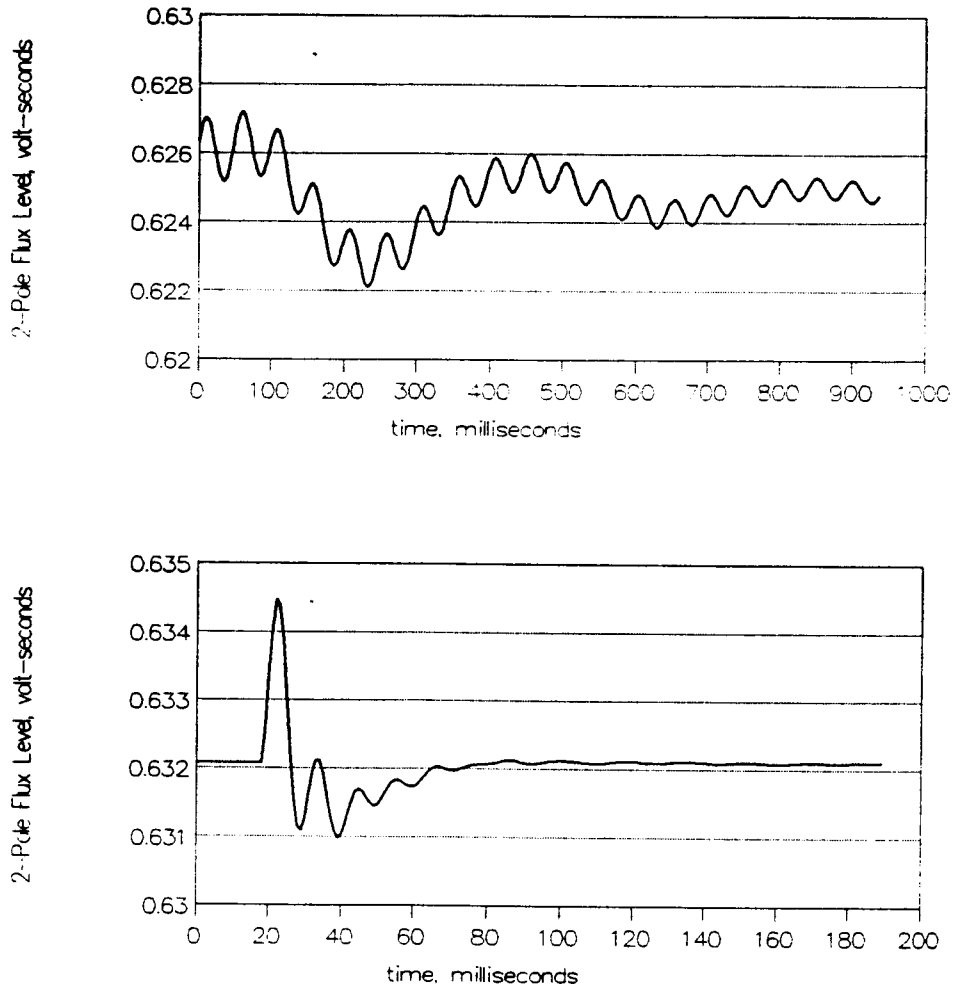


Figure 3.2: Response to Load Torque Disturbance (1 Nm step decrease at 600 r/min); 2-Pole Flux Level
a) open-loop; b) closed-loop

Figures 3.3a and 3.3b illustrate the differences between the open- and closed-loop responses, in electrical torque, to the -1 Nm step change in load torque, at 600 r/min. These figures show the true "step response" of the system; that is, the electrical torque is intended to directly follow the step change in the load torque. In the open loop, the step response has roughly 50% overshoot, and the oscillations last for over 1 second. In the closed loop, the step response has roughly 45% overshoot, which is

nearly as much, but the oscillations last only 60 ms. It should be noted that the step response in the closed loop is largely a function of the 6 gains (a-f) shown in the PI section of the Controller Block Diagram, Figure 2.1. By carefully adjusting these, the rise time, overshoot, and oscillatory behavior of the closed-loop step response may be fine-tuned. (The fine-tuning process has not been completed at this time, but will be the focus of future research.)

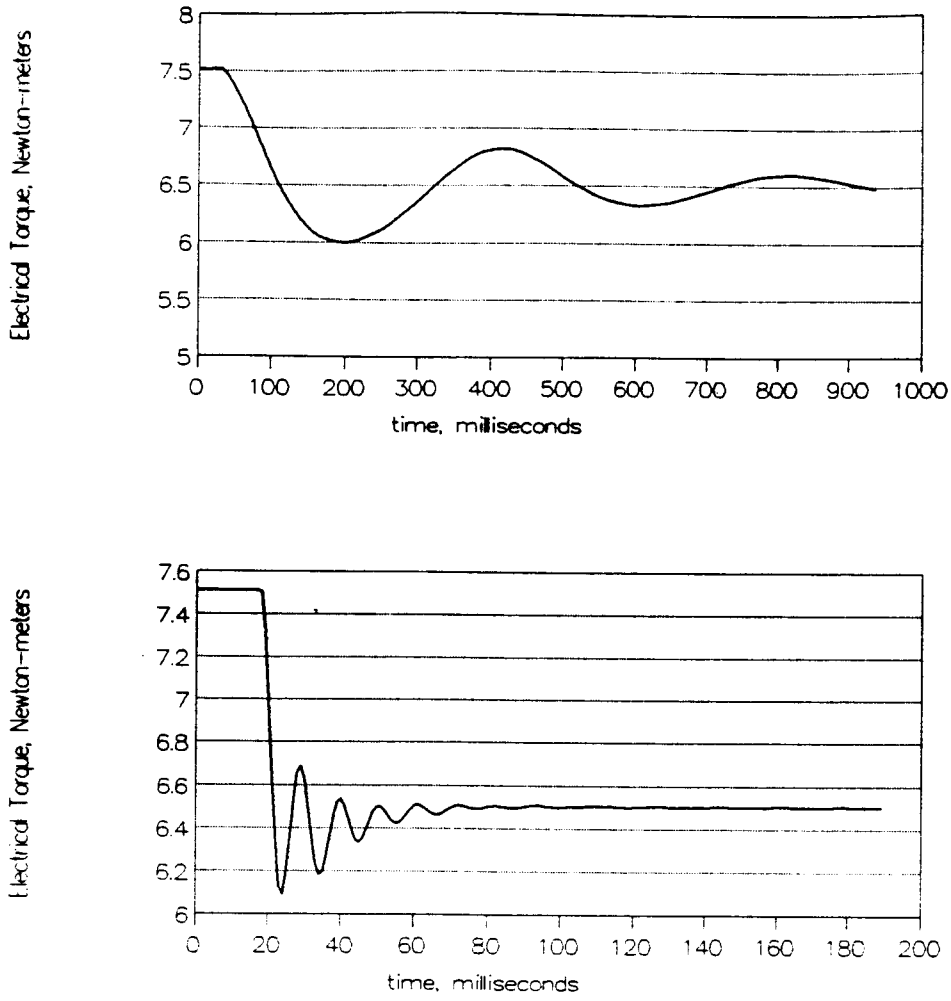


Figure 3.3: Response to Load Torque Disturbance (1 Nm step decrease at 600 r/min); Electrical Torque
a) open-loop; b) closed-loop

Figures 3.4a and 3.4b illustrate the differences between the open- and closed-loop responses, in shaft speed, to a -1 Nm step change in load

torque, at 1500 r/min. It is immediately apparent that these two figures are nearly identical to Figures 3.1a and 3.1b; the only significant difference is the offset of 900 r/min between the two sets of figures. The open- and closed-loop rise times, overshoots, and decay times are virtually identical and need not be repeated here.

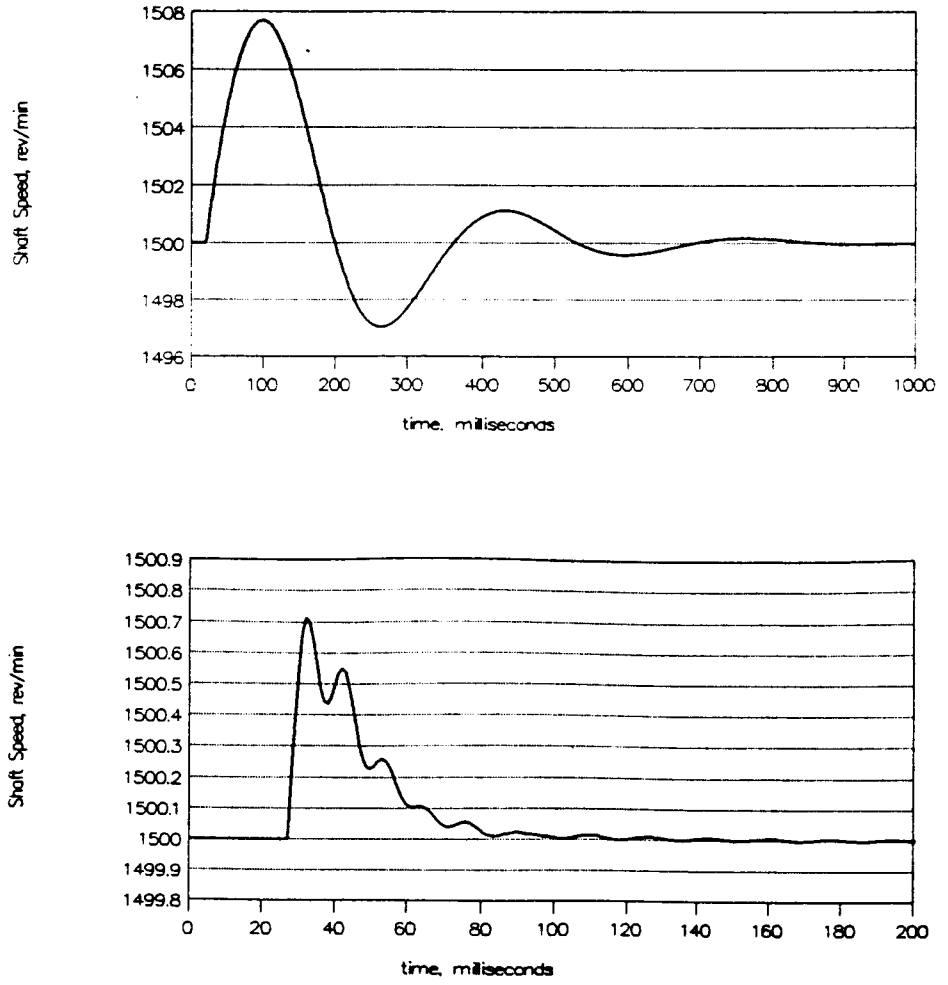


Figure 3.4: Response to Load Torque Disturbance (1 Nm step decrease at 1500 r/min); Shaft Speed
a) open-loop; b) closed-loop

Figures 3.5a and 3.5b illustrate the differences between the open- and closed-loop responses, in 2-pole flux level, to the -1 Nm step change in load torque, at 1500 r/min. Here, the open-loop transient and oscillation is smaller than that of the closed-loop transient and oscillation, by roughly

a factor of 10. The closed-loop oscillation has a shorter duration, however, by roughly a factor of 10. In both cases, the flux transient is negligible compared to the total flux magnitude; therefore, any differences between open- and closed-loop performance are moot.

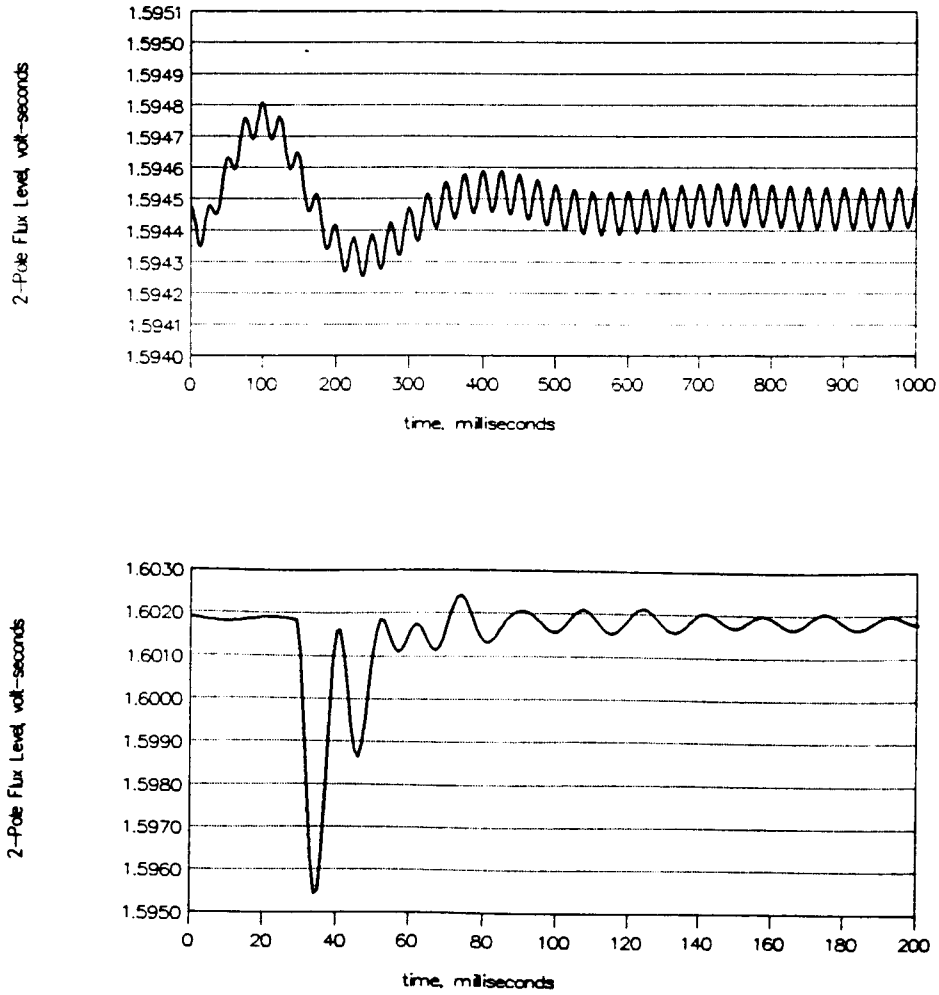


Figure 3.5: Response to Load Torque Disturbance (1 Nm step decrease at 1500 r/min); 2-Pole Flux Level
a) open-loop; b) closed-loop

Figures 3.6a and 3.6b illustrate the differences between the open- and closed-loop responses, in electrical torque, to the -1 Nm step change in load torque, at 1500 r/min. Once again, the responses at 1500 r/min are virtually identical to those at 600 r/min, with only minor differences in overshoot and settling time.

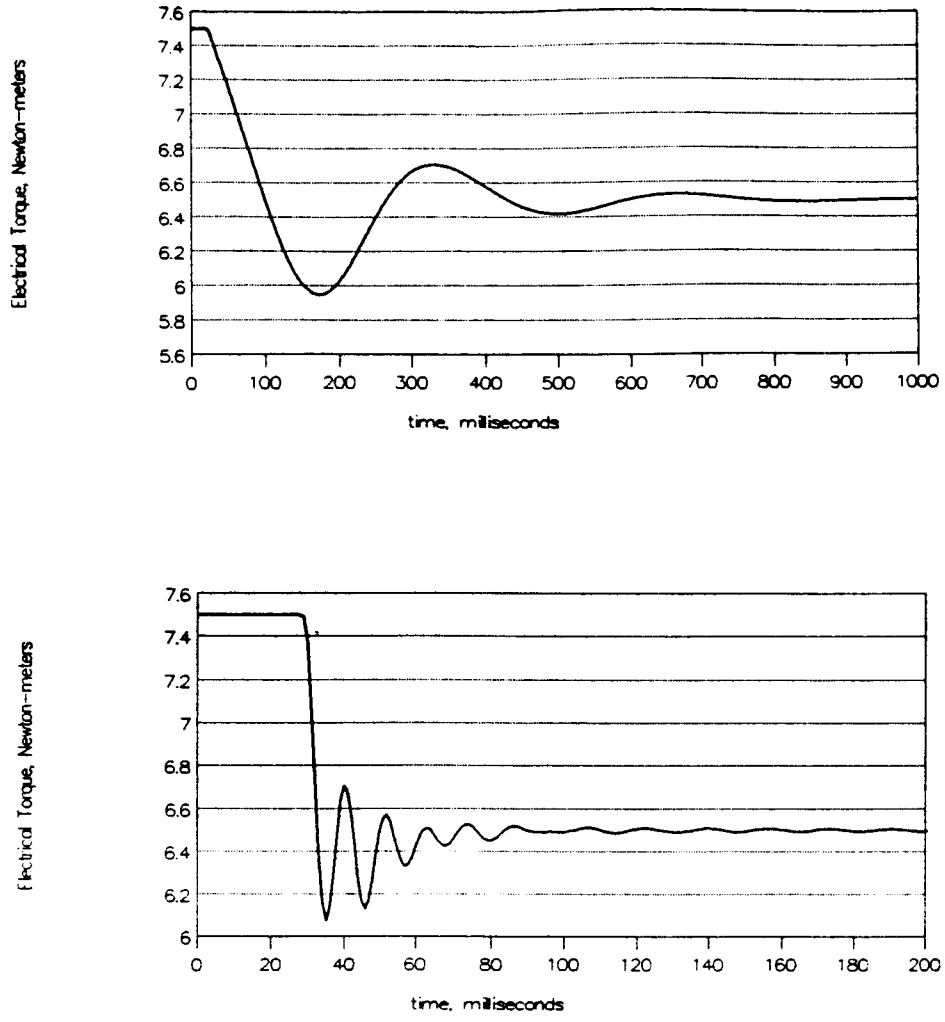


Figure 3.6: Response to Load Torque Disturbance (1 Nm step decrease at 1500 r/min); Electrical Torque
a) open-loop b) closed-loop

Figures 3.7a and 3.7b illustrate the differences between the open- and closed-loop responses, in shaft speed, to a +100 r/min step change in command speed. In both tests, the BDFM is operating in the steady-state, at maximum efficiency 2-pole flux level, with a 7.5 Nm load torque, and at a speed of 600 r/min, before the step is applied. The steady-state flux level is maintained throughout the transient. In the open-loop, the step change in command speed is given by a step change in the 2-pole excitation frequency, with a corresponding 2-pole voltage increase which will maintain the desired flux level. The shaft speed of the BDFM increases to the desired

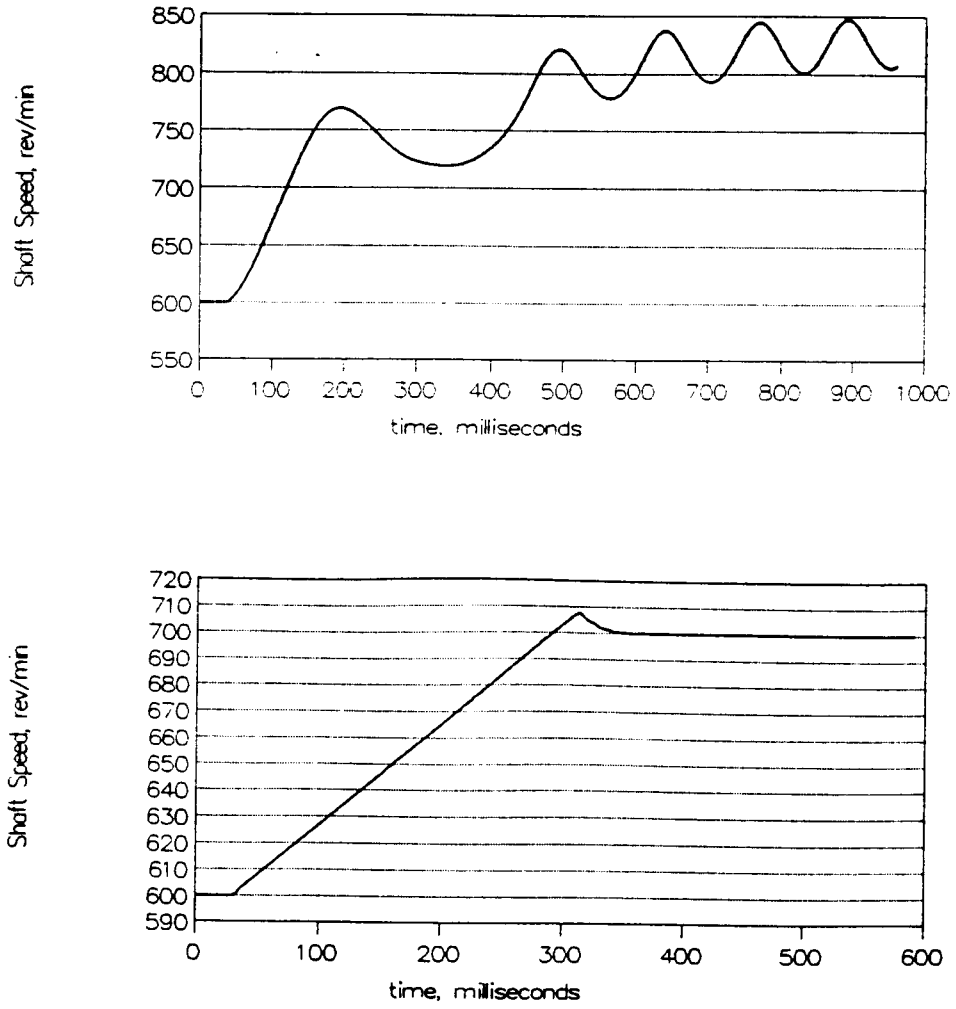


Figure 3.7: Response to Step Change in Speed Command (+100 r/min increase from 600 r/min); Shaft Speed
a) open-loop; b) closed-loop

700 r/min, and then overshoots to roughly 770 r/min; at this point, the speed takes a dip at roughly 725 r/min and then goes into a large oscillation centered at 825 r/min, where it remains. The BDFM is no longer operating synchronously but instead is operating in an unstable combination of induction modes. In the closed-loop, the shaft speed of the BDFM accelerates uniformly to 700 r/min, overshoots slightly (by about 8 r/min), and then quickly settles back down to 700 r/min. Uniform acceleration is achieved with a torque limiter, not shown in the Controller Block Diagram (Figure 2.1).

Figures 3.8a and 3.8b illustrate the differences between the open- and closed-loop responses, in 2-pole flux level, to the +100 r/min step change in command speed. In the open loop, the flux level varied erratically in a large, uncontrolled oscillation, indicating extreme system instability; total peak-to-peak flux deviation was approximately 0.2 volt-seconds, centered around 0.55 volt-seconds. In the closed loop, the flux level experiences only minor transients and maintains a constant 0.632 volt-seconds, with a peak-to-peak deviation of only 0.0125 volt-seconds. Transient decay is very fast, on the order of 50 ms.

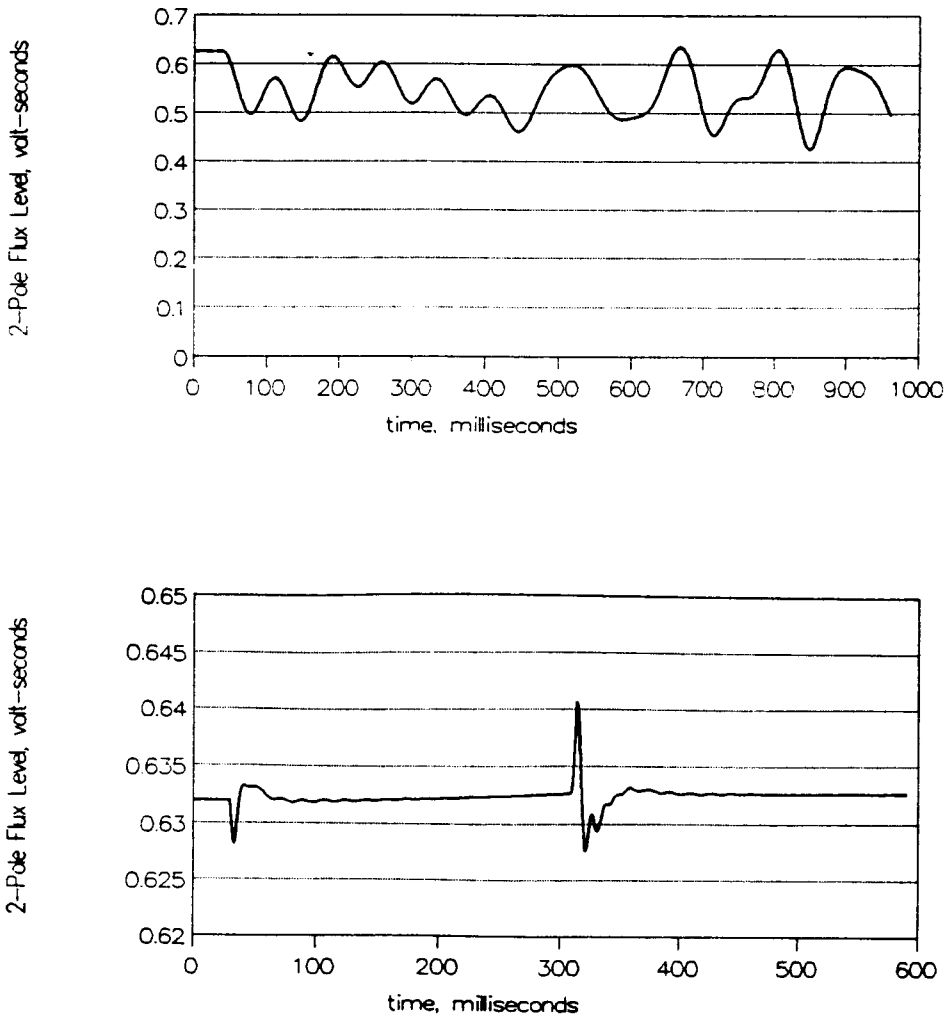


Figure 3.8: Response to Step Change in Speed Command (+100 r/min increase from 600 r/min); 2-Pole Flux Level
a) open-loop; b) closed-loop

Figures 3.9a and 3.9b illustrate the differences between the open- and closed-loop responses, in shaft speed, to a +100 r/min step change in command speed, starting at 1500 r/min. In both tests, the BDFM is operating in the steady-state, at maximum efficiency 2-pole flux level, with 7.5 Nm of load torque, before the step is applied. The steady-state flux level is maintained throughout the response transient. In the open-loop, the step change in command speed is given by a step change in the 2-pole excitation frequency, with a corresponding 2-pole voltage increase to maintain the desired flux level. The shaft speed of the BDFM increases to roughly 1540 r/min and then falls back into a combination of induction modes, oscillating

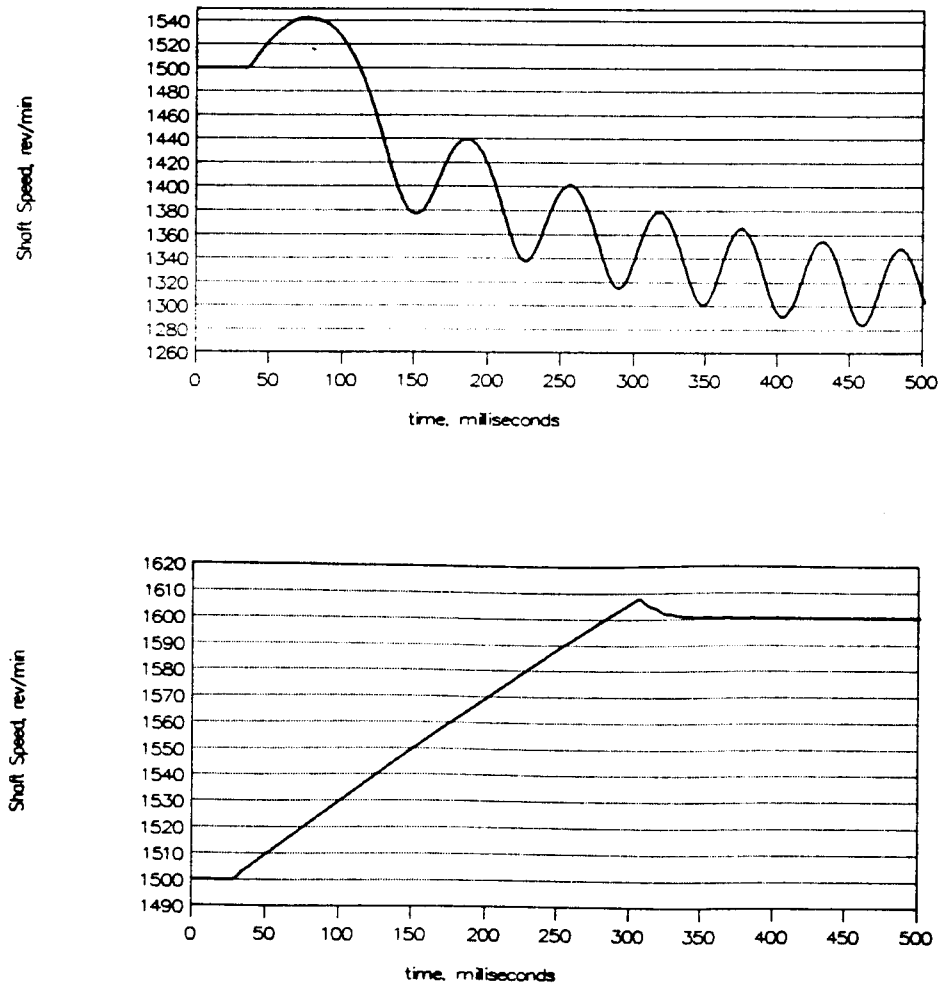


Figure 3.9: Response to Step Change in Speed Command (+100 r/min increase from 1500 r/min); Shaft Speed
a) open-loop; b) closed-loop

near 1300 r/min. In the closed loop, the shaft speed of the BDFM accelerates uniformly to 1600 r/min, overshoots slightly (by about 8 r/min), and then quickly settles to 1600 r/min. Uniform acceleration is achieved with a torque limiter, not shown in the Controller Block Diagram (Figure 2.1).

Figures 3.10a and 3.10b illustrate the differences between the open- and closed-loop responses, in 2-pole flux level, to the +100 r/min step change in command speed. In the open loop, the flux level experiences peak-to-peak deviations of 0.05 volt-seconds, centered around 1.605 volt-seconds; this is actually an unexpectedly small deviation, considering that the BDFM

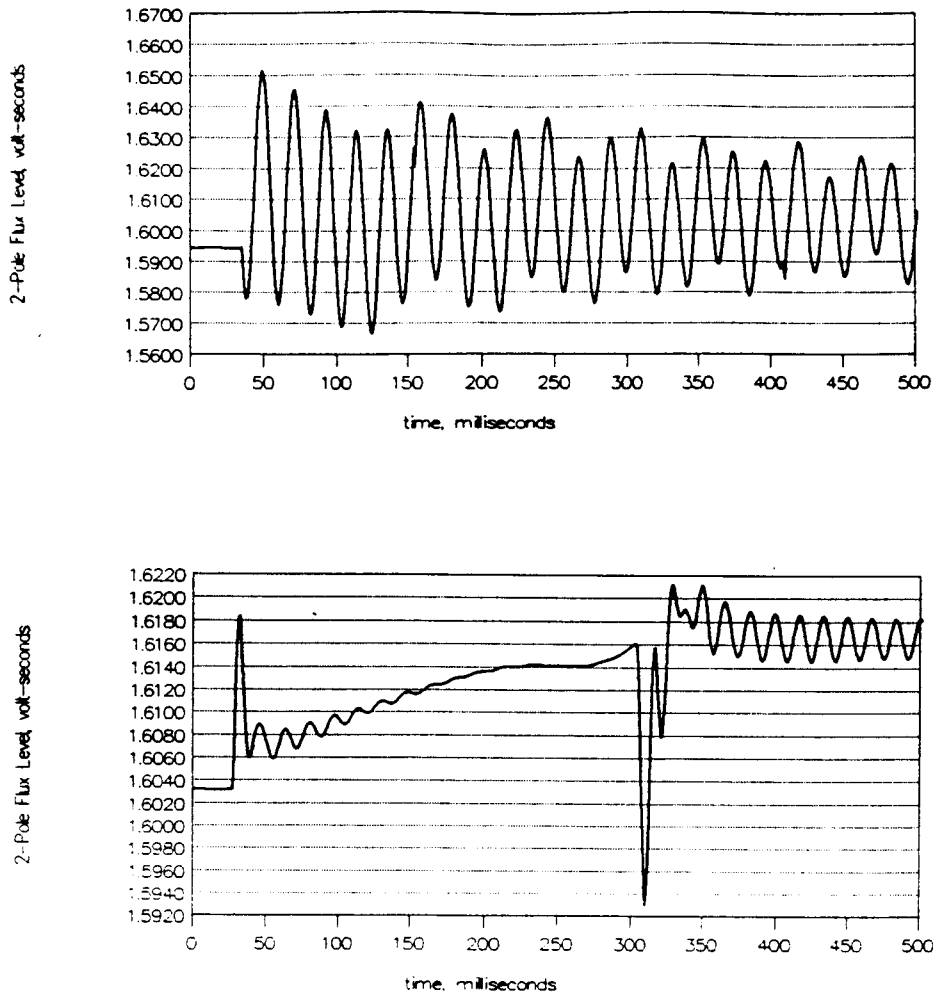


Figure 3.10: Response to Step Change in Speed Command (+100 r/min increase from 1500 r/min); 2-Pole Flux Level
a) open-loop; b) closed-loop

has become "unstable" and is no longer operating synchronously. In the closed loop, the flux level's total peak-to-peak deviation is approximately 0.028 volt-seconds; at the end of the speed transition, the flux level increases to 1.6165 volt-seconds from 1.603 volt-seconds, a 0.0135 volt-second change. The most likely explanantion for this is that two slightly different versions of 2-pole flux level are being compared. The controller's function is to regulate the predicted flux level so that it matches that of the command value. The flux level data captured by the simulator and exported to Quattro for plotting is that of the present-time; it is the actual flux level of the BDFM.

## 3.2 Steady-State Performance, Open vs. Closed Loop

In the steady-state, the main performance criteria for the BDFM are efficiency and power factor. Assuming that the 6-pole excitation is fixed (unchangeable), the efficiency and power factor at a given shaft speed and load torque are determined only by the 2-pole flux level. In essence, the 2-pole flux level for the BDFM performs the same function as the DC excitation in a conventional synchronous machine; it has no effect on the shaft speed (as long as synchronous operation is maintained) but has a profound effect on the efficiency and power factor of the machine. Indeed, synchronous machines running at no load may be used as variable reactors, with a lagging power factor at low DC excitation and a leading power factor at high DC excitation; the same is true for the 2-pole excitation in the BDFM.

It has been determined that the efficiency of the BDFM is not a function of whether it is operating in open- or closed-loop; rather, it depends only on shaft speed, load torque, and 2-pole excitation. In the event that the BDFM is open-loop stable for a given operating point, closing the loop may enhance dynamic response but will have no effect on the efficiency, power factor, or any other steady-state quantity. Furthermore, it has been found that over most of the operating range, the maximum efficiency flux

level for a given shaft speed and load torque lies within the open-loop stable region, typically near the lowest possible flux level which will support the load torque. Thus, the method of Direct Torque Control, or any other method of control, can do nothing to improve the efficiency of the machine under such conditions. The BDFM under study does have some narrow bands of shaft speed (between 850 and 1050 r/min, at low load torques) at which the machine is unstable in the open loop (at the desired flux levels) and can not be operated at maximum efficiency. In these specific instances, the Direct Torque Controller provides the necessary stability to operate the machine at maximum efficiency, and greatly improves the dynamic response.

### 3.3 Controller Robustness

The controller developed in this thesis has been demonstrated as successful in numerous simulations; it has widened the stable operating region of the machine and has greatly improved dynamic response. To be of any practical value, however, a controller must also demonstrate robustness with respect to the required machine parameters, whether they are determined off-line or on-line. Without such robustness, the controller may fail when given slightly erroneous machine parameters; an exceptionally poor controller may fail even when given a "good set" of machine parameters, if the machine parameters are subject to change due to temperature, magnetic nonlinearities, skin-effect, and other secondary effects.

Off-line identification of machine parameters is perhaps the most important aspect to consider; the controller uses these parameters to model the dynamics of the BDFM. All together, the BDFM has 11 parameters describing its electrical system, as listed in Appendix A. (The mechanical system also has parameters such as rotor moment of inertia and frictional damping factor, but these are also load-dependent and will not be discussed here.) Most of these parameters may be easily measured by simple procedures at the terminals of the machine; $r_6$ and $r_2$, for example, may be measured with a good ohmmeter,

or if necessary, a Wheatstone Bridge. $L_{m6}$, $L_{m2}$, $L_{l6}$, and $L_{l2}$ may be measured without difficulty in a blocked-rotor test of the machine. The more difficult quantities to measure are M6, M2, $r_r$, $L_{mr}$, and $L_{lr}$, because these can not be measured directly. The machine must be subjected to more rigorous and complicated tests, and advanced mathematical techniques [14,15] are required to extract the parameters from the raw data. Significant error may be introduced into the estimation process of these parameters, because of the mathematical complexity of the procedures involved. For this reason, extensive simulations were performed, analyzing the effects of errors in these parameters. (M6, M2, $r_r$, $L_{lr}$ were tested; $L_{mr}$ was not tested.)

Table 3.1: Controller Robustness Ranges, with respect to Static Machine Parameters

| Machine Parameter | Useful Error Range | Maximum Error Range |
|---|---|---|
| M6 | [-20% , +2%] | [-40% , +4%] |
| M2 | [-3.9% , +0.8%] | [-5% , +1%] |
| $r_r$ | [-60% , +15.1%] | [-100% , +45%] |
| $L_{lr}$ | [-1.8% , +15.9%] | [-3% , +23%] |

(The operating conditions are 1500 r/min, 7.5Nm load torque, and maximum possible efficiency. V6 = 230 V, h = 0.0001, BDFMDAT5.BLK machine parameters. Simulated with RBSTCHK1.PAS, which uses RBSTSUB1.PAS. (See Appendix J for description of these programs; see Appendix A for machine parameters.) Step change in load torque, down to 6.5 Nm, as well as +100 r/min step change, are performed to test the response of the controller.) All other machine parameters were left the same for this test.

The controller appears to be "robust" with respect to M6, with good performance in the "useful error range"; that is, the controller's dynamic response has acceptable rise time, overshoot, and oscillatory characteristics. Overestimates of M6 are not very well tolerated by the controller; however, it is quite forgiving of underestimates of M6, as can be seen by the asymmetrical "useful error range" interval in Table 3.1. The maximum error range is seen to be twice the width of the useful range; in this interval, the controller maintains stable operation of the BDFM but does allow limit cycles in the steady-state. Dynamic response in this interval is fair to poor outside the "useful" error range. Outside this interval, the closed-loop operation

of the BDFM is not possible because the behavior of the voltage control matrix, as observed by its determinant, is unstable. The width of the "useful" error range is 22% of the actual value of M6; this implies a useful measurement tolerance of ±11%, which seems easily obtainable. Measurement error in M6 is not expected to be a cause for concern in controller operation, especially if it is underestimated slightly.

With respect to M2, the controller is considerably less robust, with the width of the useful range being only 4.7%. This implies a maximum measurement tolerance of ±2.35%, which is difficult to obtain, especially considering that M2 can not be directly measured. The controller is probably more sensitive to error in M2 than it is to error in M6 because M2 is more intimately involved with the control of the BDFM; it couples the power converter's output voltage directly to the rotor, while M6 is only indirectly involved. In any case, M2 will have to be determined with extreme care. It may be necessary to fine-tune the value of M2, to optimize the controller's performance; perhaps this iterative process could be automated by the controller.

The controller displayed remarkable robustness with respect to the machine parameter $r_r$, the rotor resistance, with a useful error range width of 75.1%, indicating a very generous measurement tolerance of ±37.55%. This is important, for three reasons: First, the rotor resistance can not be measured directly, and the estimation process is expected to introduce significant error. Second, $r_r$ is subject to change significantly due to temperature, as the rotor becomes quite hot (as much as 60 degrees C rise). Third, $r_r$ varies widely due to skin-effect; the doubly-fed nature of the machine induces high-frequency currents into the rotor conductors, which have a large cross-sectional area and a geometry which makes them vulnerable to this effect. Indeed, it is fortunate to see that the controller is very tolerant in terms of this machine parameter; it will still function when the rotor resistance is assumed to be zero.

The last machine parameter tested for robustness was $L_{lr}$, the rotor leakage inductance. The controller was reasonably tolerant of error in this quantity, with a "useful" error range width of 17.7%, which implies ±8.85% measurement tolerance for this quantity. This would be a simple matter if $L_{lr}$ could be measured directly; however, since it can't be measured directly, this error tolerance is somewhat restrictive, although not unreasonable. Careful measurement of the other more directly measureable quantities, together with careful data acquisition and analysis should yield a value of Llr with an acceptably small error.

Of all of the static machine parameters tested for robustness, $r_r$ and M6 should be of little concern. The controller has demonstrated excellent insensitivity to these parameters, and although they can't be measured directly, they should be obtainable with the required accuracy. Error in $L_{lr}$ may be a slight problem, but $L_{lr}$ should also be obtainable with the required accuracy if proper care is taken. M2 is the main cause for concern because of the controller's low tolerance for error in this quantity. For further details on the measurement procedures and difficulties for M2 and other quantities, refer to [16].

The other machine parameters ($r_6$, $r_2$, $L_{m6}$, $L_{m2}$, $L_{l6}$, $L_{l2}$, $L_{mr}$), were not tested for robustness but could have similar problems, as exhibited by M2; the controller may be rather sensitive to errors in $L_{l6}$ and $L_{l2}$, as these affect machine performance quite noticeably. This is not expected to cause any serious problems, however, because these parameters can all be measured with a high degree of accuracy with fairly simple tests (with the exception of $L_{mr}$).

The robustness isssue has so far been addressed only with respect to the static, or off-line, machine parameters. There are many other sources of error which may adversely affect controller performance, in the dynamic, or on-line, machine parameters such as terminal voltages, line currents,

rotor position, and rotor speed. Errors on the order of ±3% to ±5% are to be expected in all of these quantities, due to noise, phase shifts, anti-aliasing filtering, and quantization. To make matters worse, some of the required quantities, such as flux levels and rotor speed, are not directly measured but are determined by processing of directly-measured quantities, by integration or differentiation. Controller robustness with respect to these parameters will be thoroughly investigated when the DSP hardware is completed.

The effects of errors in estimated 6- and 2-pole flux levels have been observed in the operation of the controller but have not been formally recorded. In order to save on the total system cost and physical complexity, the flux levels are estimated by integration of the terminal voltages, rather than by using Hall-effect sensors. This integration is performed in the stationary reference frame, as described in Equations 2.16 to 2.19. The problem with real-world integrators, however, is that they drift and eventually "saturate", either by hitting a power supply rail (analog) or overflowing an integer or floating point number (digital). To counteract this, a very slow leakage term is programmed into the integrator, with a decay constant on the order of 0.5 second. With rapidly changing flux levels, this decay constant has virtually no consequence in terms of flux error. It has a more profound effect, however, when the (stationary reference frame) flux levels are changing very slowly, especially on the 2-pole side of the machine, where low frequencies may occur. These errors may be amplified in any calculations which use flux levels as their inputs, electrical torque, for instance. Electrical torque estimation errors as high as 35% have been observed as a result of the errors in the flux levels; however, the controller did manage to maintain accurate speed control of the machine in spite of these errors. (The controller ultimately uses shaft speed and acceleration data to determine the required torque changes; thus, electrical torque estimation errors, as well as load torque estimation errors, have little effect on performance.) Controller dynamic performance does suffer somewhat from flux integration leakage error, contributing to oscillatory behavior under some operating conditions.

Formal robustness analysis of on-line machine parameters is recommended for further study of this controller design. Another possible topic for the further development of the controller would be a machine-parameter estimation block, giving the controller a "self-tuning" nature and greatly improving its robustness. Such an estimation block would operate very slowly, updating the static machine parameters every few seconds or every few minutes, thus avoiding the need for "real time" speed. Another feature which could improve the controller's robustness is an adaptive outer loop to replace the simple PI controller shown in the Controller Block Diagram, Figure 2.1.

## 3.4 Implementation Considerations

### 3.4.1 Choice of Power Electronic Converter

All simulations referred to in this thesis have used a very simple converter model, one that operates in the controlled-voltage output mode. The output of the converter is updated once every controller-update period and is held at the desired voltage level between updates. Thus, such a converter produces a waveform representing a "sample-and-hold" function of the desired output waveform. The series-resonant current-link converter can closely approximate such a waveform, if it has a sufficiently high switching frequency. In the voltage mode, it uses hysteresis-type voltage control, using current pulses to charge the output capacitors to the desired voltage. Eventually, however, a space-vector PWM converter should be tried, both in the simulations and in the lab. In [9], a space-vector PWM converter was successfully simulated and implemented in a Direct Torque Control scheme for an induction machine.

### 3.4.2 Development of Hardware Implementation

A Motorola DSP 56001 has been chosen for the hardware implementation of the controller. It is interfaced to 7 A/D converters, 1 digital input,

and 3 D/A converters; the purposes of each appear in Table 3.2. For a schematic of the DSP system, refer to Appendix G. It should be noted that the hardware implementation is an extension of the work presented here, and that the ongoing project has been forwarded to others. A brief description of the system is included below, however, for completeness.

Table 3.2: DSP to BDFM Transducer Interface Channels

| Channel # | Channel Type | Quantity input/output |
|---|---|---|
| 1 | A/D | 6-pole inst. voltage, $V_{ab6}$ |
| 2 | A/D | 2-pole inst. voltage, $V_{ab2}$ |
| 3 | A/D | 2-pole inst. voltage, $V_{bc2}$ |
| 4 | A/D | 6-pole inst. current, $I_{a6}$ |
| 5 | A/D | 6-pole inst. current, $I_{b6}$ |
| 6 | A/D | 2-pole inst. current, $I_{a2}$ |
| 7 | A/D | 2-pole inst. current, $I_{b2}$ |
| 8 | Digital | Shaft position encoder |
| 9 | D/A | Converter command voltage |
| 10 | D/A | Converter command frequency |
| 11 | D/A* | Converter command sequence |

*D/A channel used as pseudo-digital signal interface

All voltages and currents may be uniquely determined by only two measurements, assuming balanced three-phase quantities, with the exception of the 6-pole voltage, which requires only one channel for unique determination. This is because the 6-pole power grid magnitude is assumed known and constant. Computationally, the 6-pole voltage will have to be treated very carefully, as its measurement is more susceptible to the effects of noise. Determination of the 6-pole phase angle requires some "expensive" processing, including a data buffer and the calculation of arc-cosines from arc-tangents, neither of which are built into the DSP's instruction set. Series approximation or table lookup will be necessary. The other voltages and currents may be calculated in a simpler manner, but eventually, they (like all quantities) will need to be transformed to the rotor reference frame, and this involves extensive use of sine and cosine. In flux level determinations, square roots must also be computed, and they are also not built into the DSP instruction set. The rotor position is measured with a 14-bit shaft encoder, giving 0.02 degree resolution, which should be adequate. This signal is differentiated to determine rotor speed.

The power converter being interfaced to the controller and BDFM is a series-resonant, current-link design. The converter interface is quite cumbersome, as the instantaneous phase of the output voltage may not be directly commanded. Instead, an output frequency must be specified; the phase is a function of the integral of this quantity. The output sequence of the converter is given by a quasi-digital signal; it is determined by the value of the analog voltage applied to the converter's input channel. Thus, the abc/acb sequence selection is achieved via a D/A converter.

There are two causes for concern in the hardware implementation of the controller. The first concern is the effects of noise, nonlinearities, and other errors in the measurement process. The laboratory is a highly non-ideal environment, with imbalances in the power grid and converter outputs, nonlinearities in the magnetic core of the BDFM and in the transducers, and significant amounts of noise emitted by the converter at high frequencies because of its switching. Measurement cables, as well as the DSP, A/D, and D/A boards, will be shielded as much as possible, and their chassis grounded. The power converter, unfortunately, can not be grounded (chassis must be floating!); however, this problem has been solved by opto-coupling the D/A signals into the converter, to permit grounding of the controller. These precautions should provide adequate prevention of measurement noise; however, nonlinearities may still be present.

The second concern is the computational speed of the DSP system. The BDFM controller is computationally demanding, requiring hundreds of floating point operations for every controller period. Many of these floating point operations are irrational functions such as square roots, sin, cos, and arctangent, making it imperative that the DSP have a high floating-point speed capacity. The controller algorithm was analyzed for its computational demand, and it was estimated that it would require a minimum of roughly 500 KFLOPS for implementation. The controller algorithm was isolated and time-tested on an Everex Step 386, with 387 coprocessor, running at 20 MHz.

The computer, rated at 150 KFLOPS by a MATLAB test procedure, ran the controller algorithm in 1/3 real-time speed, indicating a minimum requirement of 450 KFLOPS for implementation. The Motorola DSP 56001 chip selected for the controller runs at 27 MHz and has a performance rating of roughly 13 MIPS and 6 MFLOPS, providing a ten-fold excess in computational capacity. Although this seems to be a comforting margin, it must be remembered that the DSP chip must also handle system overhead such as strobing the A/D, D/A converters and pre-processing the measurements, but perhaps the most significant time-consumer will be inefficiencies in the DSP programming. A C-compiler is available for the DSP 56001, but it is not very efficient in terms of producing fast, compact code; indeed, it can be a factor of 5 or 10 slower than an equivalent assembly-language program. At this time, the hardware/software implementation of the DSP controller is not complete but is continuing; refer to [17].

# Chapter 4

# Conclusions and Recommendations

## 4.1 Controller Effectiveness

It has been shown, through extensive simulation, that the method of Direct Torque Control may be successfully applied to brushless doubly-fed machines. Closed-loop dynamic performance is far superior to that of the open-loop, as shown in Chapter 3. Controller robustness with respect to the static machine parameters appears to be acceptable and easily manageable, except for M2, the 2-pole to rotor mutual inductance, which in simulation requires ±2.35% measurement accuracy. Robustness with respect to the dynamic machine parameters is not yet fully known, although simulated errors in flux estimation were observed to have only minor adverse effects on controller performance, for reasonable amounts of error. The controller is simulated successfully, using a voltage-controlled, idealized converter with a "sample-and-hold" output waveform, in which the voltage output simply changes to a new level every controller update period and is held there until the next update. Simulations with a space-vector PWM converter should be considered in future work.

## 4.2 Alternate Control Methods

At this time, it is unlikely that methods other than Direct Torque Control will be directly applied to the BDFM in the innermost loop, although such methods may be feasible. In the near future, it is expected that many control schemes will be developed for the BDFM, using Direct Torque Control as an integral part of the machine; in effect, the Direct Torque Control algorithm provides the interface between the various controllers and the BDFM. Among these control schemes are sliding mode, deadbeat, and bilinear control, to name a few; various forms of adaptive linear or nonlinear control

could also be applied. (A model-reference adaptive control is being developed in [17].) In any event, the method of Direct Torque Control would be central to the design.

### 4.3 Further Research Recommendations

The first recommendation is that the proposed control scheme be evaluated in the laboratory, using a real-time DSP system. Hardware implementation is nearing completion, and laboratory results will be included in [17].

The next recommendation is that various control methods be examined for use, outside of the Direct Torque Control loop. These include sliding mode, deadbeat, and bilinear control. Various adaptive control schemes may also be examined; many of these use linear models, allowing for simplicity in system identification and the use of Laplace and Z-transform analysis. Currently, a model-reference adaptive control scheme is being developed around the Direct Torque Control Loop, as a continuation of this project.

Another important recommendation is to improve the robustness of the controller, making it less sensitive to errors or changes in the static machine parameters, $m_{p1}$ through $m_{p11}$. An on-line machine parameter estimator could be added to the controller, working independently from the main control algorithm. It wouldn't need to operate extremely fast; it could update the machine parameter estimates every several seconds, or every minute. Most machine parameter changes will be due to temperature, and this would have a time constant on the order of minutes. Skin-effect in the rotor may cause fluctuations in rotor resistance. Rotor resistance will be a function of the frequency of the induced currents on the rotor, and these in turn are a function of the 2-pole excitation frequency (and thus rotor speed). Rotor resistance measurements could be taken at various rotor speeds, and these could be stored in memory for future reference. Skin-effect is not a simple thing to analyze, however, because different harmonics on the

rotor will experience different rotor resistances. These can not be accurately lumped together into a single quantity, $r_r$. Fortunately, the controller is extremely robust with respect to this parameter, and a single lumped estimate should be sufficient.

Another important issue to investigate is the 1200 r/min speed barrier. At exactly 1200 r/min, the BDFM is unable to produce any electrical torque, either open- or closed-loop. (Refer to Section 1.2 for a complete explanation.) The 1200 r/min barrier presents a significant problem in the BDFM motoring mode, because it makes the useful 1300-1800 r/min range inaccessible through conventional run-up. It would be desirable to develop a closed-loop algorithm by which the 1300-1800 speed range could be accessed, with or without a mechanical load. While no-load start-up control via the converter seems feasible, high-speed synchronization with applied load torque is not possible, given the machine characteristics and converter rating limitations.

Other pole combinations (besides 6 and 2 pole) may also be investigated, to optimize the desired speed range of the machine. Such machines would have similar mathematical model structures, but the simulators and controllers for such machines would need to be customized for the particular pole combinations. The 1200 r/min speed barrier could be broken by use of a different pole combination; however, the barrier would still exist, at a different speed.

Yet another area for further research is the adaptation of Direct Torque Control to BDFM generator applications, for use in wind turbines. This is being investigated in [18].

One final issue to be discussed is that of power converter requirements. It should be noted that the power converter's volt-ampere rating is a function of the BDFM and its intended load, and not a function of the control algorithm used. In the steady-state, the converter will deliver the same voltage and current to the machine, regardless of controller design, as long as

the same speed, load torque, and 2-pole flux level are maintained. The control algorithm is effectively transparent to the steady-state operation of the machine.

Under dynamic conditions, the control algorithm will make some difference in the power converter requirement, but again, it will be mainly a function of the BDFM and its load. Different controllers will have different acceleration and flux-level characteristics under dynamic conditions, and dynamic power converter limitations must be considered when changing speeds in the machine. Acceleration limiters may be necessary in the control loops to be sure that the power converter's maximum rated output is not exceeded. 2-pole flux level must be constantly monitored, in order to provide the necessary torque with a minimum of converter output.

# BIBLIOGRAPHY

[1] L.J. Hunt, "A New Type of Induction Motor", IEE Journal, 1921, Vol. 59, pp 648-677.

[2] F. Creedy, "Some Developments in Multi-Speed Cascade Induction Motors", IEE Journal, 1921. Vol 59, pp 511-521.

[3] A.R. Broadway and L. Burbridge, "Self-Cascaded Machine: A Low Speed Motor or High-Frequency Brushless Alternator", IEE Proceedings, 1970, 117(7), pp. 1277-1290

[4] R. Li, A.K. Wallace, and R. Spee, "Determination of Converter Control Algorithms for Stable Brushless Doubly-Fed Drives Using Floquet and Lyapunov Techniques", IEEE PESC, pp. 571-577, 1991.

[5] M. Depenbrock, "Direct Self Control (DSC) of Inverter-Fed Induction Machines", IEEE Trans. Power Electronics, vol. 3, no. 4, pp. 420-429, 1988.

[6] I. Takahashi and T.Noguchi, "A New Quick-Response and High-Efficiency Control Strategy of an Induction Motor", IEEE Trans. IAS, vol. IA-22, no. 5, pp. 820-827, 1986

[7] I. Boldea and J.A. Trica, "Torque Vector Controlled (TVC) Voltage-Fed Induction Motor Drives -- Very Low Speed Performance via Sliding Mode Control", International Conf. on Elect. Machines, pp. 1212-1217, 1990.

[8] A. Sabanovic and F. Bilalovic, "Sliding Mode Control of AC Drives", IEEE Trans. IAS, Vol IA-25, no. 1, pp. 70-75, 1989.

[9] T.G. Habetler, F. Profumo, M. Pastorelli, and L.M. Tolbert, "Direct Torque Control of Induction Machines Using Space Vector Modulation", IEEE-IAS Annual Meeting Conference Record, pp. 428-436, 1991.

[10] W.R. Brassfield, R. Spee, T.G. Habetler, "Direct Torque Control for Brushless Doubly-Fed Machines", IEEE-IAS Annual Meeting Conference Record, pp. 615-622, 1992.

[11] V.S. Javadekar, "Design and Development of a Controller for a Brushless Doubly-Fed Automotive Alternator System", M.S. Thesis, Oregon State University, January 1992.

[12] R. Li, "Dynamic Modeling, Simulation, and Stability Analysis of Brushless Doubly-Fed Machines", Ph.D. Dissertation, Oregon State University, May 1991.

[13] R. Li, A.K. Wallace, and R. Spee, "Two-Axis Model Development of Cage-Rotor Brushless Doubly-Fed Machines", IEEE Trans. Energy Conversion, vol. 6, no. 3, pp. 453-460, 1991.

[14] G.C. Alexander, A. Ramchandran, R. Spee, and A.K. Wallace, "Parameter Identification for Brushless Doubly-Fed Synchronous Machines", International Conference on the Evolution and Modern Aspects of Synchronous Machines, pp. 126-131, Zurich, Switzerland, August 1991.

[15] A. Ramchandran, G.C. Alexander, " Frequency-Domain Parameter Estimation for the Brushless Doubly-Fed Machine", Power Conversion Conference-Yokohama, Yokohama, Japan, April 1993.

[16] A. Ramchandran, "Parameter Estimation for the Brushless, Doubly-Fed Machine", Ph.D. Dissertation, Oregon State University, expected 1993.

[17] D. Zhou, "Model-Reference Adaptive Control for Brushless Doubly-Fed Machines", Ph.D. Dissertation, Oregon State University, in progress.

[18] C. Brune, "Direct Torque Control for BDFM Generator Applications", M.S. Thesis, Oregon State University, in progress.

[19] P. Rochelle, "Design and Analysis of the Brushless Doubly-Fed Machine", M.S. Thesis, Oregon State University, 1990.

# APPENDICES

# Appendix A

## BDFM Machine Parameters Legend

In the following machine parameters, all quantities are expressed in terms of standard SI units. The numbers shown here represent the machine specifically under study (the lab prototype):

| | | | |
|---|---|---|---|
| 6-pole magnetizing inductance | ($L_{m6}$) | = | 0.0679 H |
| 6-pole leakage inductance | ($L_{l6}$) | = | 0.012 H |
| 6-pole to rotor mutual inductance | ($M_6$) | = | 0.00088692 H |
| rotor magnetizing inductance | ($L_{mr}$) | = | 0.000020833 H |
| rotor leakage inductance | ($L_{lr}$) | = | 0.000020833 H |
| 6-pole winding resistance | ($r_6$) | = | 0.80667 ohms |
| rotor conductor resistance | ($r_r$) | = | 0.001572 ohms |
| 2-pole magnetizing inductance | ($L_{m2}$) | = | 0.61921 H |
| 2-pole leakage inductance | ($L_{l2}$) | = | 0.012 H |
| 2-pole to rotor mutual inductance | ($M_2$) | = | 0.0043042 H |
| 2-pole winding resistance | ($r_2$) | = | 0.80667 ohms |
| rotor moment of inertia | (J) | = | 0.05 kg*m^2 |

| | | |
|---|---|---|
| 6-pole frequency | = | 60 Hz |
| 6-pole voltage (line-line RMS) | = | 230 V |

# Appendix B

## BDFM Variables Legend

**State Variables:**

$i_{q6}$, $i_{d6}$, $i_{06}$: q, d, and 0 components of 6-pole stator currents

$i_{q2}$, $i_{d2}$, $i_{02}$: q, d, and 0 components of 2-pole stator currents

$i_{qr}$, $i_{dr}$, $i_{0r}$: q, d, and 0 components of rotor currents

$\theta_r$, $\omega_r$: shaft angle, shaft angular velocity ($\omega_r$ is also the system "output")

**Electrical Torques:**

$t_{e6} = 3M_6(i_{q6}i_{dr} - i_{d6}i_{qr})$ = 6-pole torque component (B1)

$t_{e2} = M_2(i_{q2}i_{dr} + i_{d2}i_{qr})$ = 2-pole torque component (B2)

$t_e = t_{e6} + t_{e2}$ = total electrical torque (B3)

$t_l$ = load torque

**Forcing Function:**

$v_{q6}$, $v_{d6}$, $v_{06}$: q, d, and 0 components of 6-pole stator voltage from power grid

$v_{q2}$, $v_{d2}$, $v_{02}$: q, d, and 0 components of 2-pole stator voltage from power converter

$v_{qr}$, $v_{dr}$, $v_{0r}$: q, d, and 0 components of rotor voltage (zero; short-circuited)

**ABC Quantities:**

$v_{a6}$, $v_{b6}$, $v_{c6}$: 6-pole line-to-neutral voltages

$v_{a2}$, $v_{b2}$, $v_{c2}$: 2-pole line-to-neutral voltages

$i_{a6}$, $i_{b6}$, $i_{c6}$: 6-pole abc line currents

$i_{a2}$, $i_{b2}$, $i_{c2}$: 2-pole abc line currents

**Unused Quantities:**

$i_{06}$, $i_{02}$, $i_{0r}$, $v_{06}$, $v_{02}$, $v_{0r}$ don't appear in the equations because balanced 3-phase is assumed.

**Coordinate Transformations:**

**Voltage Transformation (abc to qd0):**

$$v_{q6} = \text{sqrt}(2/3)[v_{a6}\cos(3\theta_r) + v_{b6}\cos(3\theta_r-2\pi/3) + v_{c6}\cos(3\theta_r+2\pi/3)] \quad \text{(B4)}$$

$$v_{d6} = \text{sqrt}(2/3)[v_{a6}\sin(3\theta_r) + v_{b6}\sin(3\theta_r-2\pi/3) + v_{c6}\sin(3\theta_r+2\pi/3)] \quad \text{(B5)}$$

$$v_{q2} = \text{sqrt}(2/3)[v_{a2}\cos(\theta_r-2\pi/9) + v_{b2}\cos(\theta_r-2\pi/9-2\pi/3) + v_{c2}\cos(\theta_r-2\pi/9+2\pi/3)] \quad \text{(B6)}$$

$$v_{d2} = \text{sqrt}(2/3)[v_{a2}\sin(\theta_r-2\pi/9) + v_{b2}\sin(\theta_r-2\pi/9-2\pi/3) + v_{c2}\sin(\theta_r-2\pi/9+2\pi/3)] \quad \text{(B7)}$$

Note: $v_{06}$ and $v_{02}$ are zero because a balanced 3-phase system is assumed

**Current Transformation (qd0 to abc):**

$$i_{a6} = \text{sqrt}(2/3)[i_{q6}\cos(3\theta_r) + i_{d6}\sin(3\theta_r)] \quad \text{(B8)}$$

$$i_{b6} = \text{sqrt}(2/3)[i_{q6}\cos(3\theta_r-2\pi/3) + i_{d6}\sin(3\theta_r-2\pi/3)] \quad \text{(B9)}$$

$$i_{c6} = \text{sqrt}(2/3)[i_{q6}\cos(3\theta_r+2\pi/3) + i_{d6}\sin(3\theta_r+2\pi/3)] \quad \text{(B10)}$$

$$i_{a2} = \text{sqrt}(2/3)[i_{q2}\cos(\theta_r-2\pi/9) + i_{d2}\sin(\theta_r-2\pi/9)] \quad \text{(B11)}$$

$$i_{b2} = \text{sqrt}(2/3)[i_{q2}\cos(\theta_r-2\pi/9-2\pi/3) + i_{d2}\sin(\theta_r-2\pi/9-2\pi/3)] \quad \text{(B12)}$$

$$i_{c2} = \text{sqrt}(2/3)[i_{q2}\cos(\theta_r-2\pi/9+2\pi/3) + i_{d2}\sin(\theta_r-2\pi/9+2\pi/3)] \quad \text{(B13)}$$

Note: Again, a balanced 3-phase system is assumed

# Appendix C

## BDFM Equations in Simulator Notation

**System Differential Equations (8th-order):**

$$dy_1/dt = y_{11}(3L_{1,1}AA_{1,8}+L_{1,4}AA_{4,8})y_8 + y_{11}(3A_{1,2}y_2+A_{1,5}y_5) - L_{1,1}x_1 + A_{1,1}y_1 + A_{1,4}y_4 + A_{1,7}y_7 - L_{1,4}x_4 \quad (C1)$$

$$dy_2/dt = -y_{11}(3L_{2,2}AA_{2,7}+L_{2,5}AA_{5,7})y_7 - y_{11}(3A_{2,1}y_1+A_{2,4}y_4) + L_{2,2}x_2 + A_{2,2}y_2 + A_{2,5}y_5 + A_{2,8}y_8 - L_{2,5}x_5 \quad (C2)$$

$$dy_4/dt = y_{11}(3L_{4,1}AA_{1,8}+L_{4,4}AA_{4,8})y_8 + y_{11}(3A_{4,2}y_2+A_{4,5}y_5) - L_{4,4}x_4 + A_{4,1}y_1 + A_{4,4}y_4 + A_{4,7}y_7 - L_{4,1}x_1 \quad (C3)$$

$$dy_5/dt = -y_{11}(3L_{5,2}AA_{2,7}+L_{5,5}AA_{5,7})y_7 - y_{11}(3A_{5,1}y_1+A_{5,4}y_4) + L_{5,5}x_5 + A_{5,2}y_2 + A_{5,5}y_5 + A_{5,8}y_8 - L_{5,2}x_2 \quad (C4)$$

$$dy_7/dt = y_{11}(3L_{7,1}AA_{1,8}+L_{7,4}AA_{4,8})y_8 + y_{11}(3A_{7,2}y_2+A_{7,5}y_5) - L_{7,1}x_1 + A_{7,1}y_1 + A_{7,4}y_4 + A_{7,7}y_7 - L_{7,4}x_4 \quad (C5)$$

$$dy_8/dt = -y_{11}(3L_{8,2}AA_{2,7}+L_{8,5}AA_{5,7})y_7 - y_{11}(3A_{8,1}y_1+A_{8,4}y_4) + L_{8,2}x_2 + A_{8,2}y_2 + A_{8,5}y_5 + A_{8,8}y_8 - L_{8,5}x_5 \quad (C6)$$

$$dy_{10}/dt = y_{11} \quad (C7)$$

$$dy_{11}/dt = (t_e - t_l)/JJ \quad (C8)$$

**State Variables:**

$y_1$, $y_2$, $y_3$: q, d, and 0 components of 6-pole stator currents
$y_4$, $y_5$, $y_6$: q, d, and 0 components of 2-pole stator currents
$y_7$, $y_8$, $y_9$: q, d, and 0 components of rotor currents
$y_{10}$, $y_{11}$: shaft angle, shaft angular velocity ($y_{11}$ is also the system "output")

**Electrical Torques:**

$$t_{e6} = 3m_{p3}(y_1y_8-y_2y_7) = \text{6-pole torque component} \quad (C9)$$

$$t_{e2} = m_{p10}(y_4y_8+y_5y_7) = \text{2-pole torque component} \quad (C10)$$

$$t_e = t_{e6} + t_{e2} = \text{total electrical torque} \quad (C11)$$

$t_l$ = load torque

**Forcing Function:**

$x_1$, $x_2$, $x_3$: q, d, and 0 components of 6-pole stator voltage from power grid

$x_4$, $x_5$, $x_6$: q, d, and 0 components of 2-pole stator voltage from power converter

$x_7$, $x_8$, $x_9$: q, d, and 0 components of rotor voltage (zero; short-circuited)

**ABC Quantities:**

$v_a$, $v_b$, $v_c$: 6-pole line-to-neutral voltages

$u_a$, $u_b$, $u_c$: 2-pole line-to-neutral voltages

$i_1$, $i_2$, $i_3$: 6-pole abc line currents

$i_4$, $i_5$, $i_6$: 2-pole abc line currents

**Unused Quantities:**

$y_3$, $y_6$, $y_9$, $x_3$, $x_6$, $x_9$ don't appear in the equations because balanced 3-phase is assumed.

**Coordinate Transformations:**

**Voltage Transformation (abc to qd0):**

$$x_1 = \text{sqrt}(2/3)[v_a\cos(3y_{10}) + v_b\cos(3y_{10}-2\pi/3) + v_c\cos(3y_{10}+2\pi/3)] \quad \text{(C12)}$$

$$x_2 = \text{sqrt}(2/3)[v_a\sin(3y_{10}) + v_b\sin(3y_{10}-2\pi/3) + v_c\sin(3y_{10}+2\pi/3)] \quad \text{(C13)}$$

$$x_4 = \text{sqrt}(2/3)[u_a\cos(y_{10}-2\pi/9) + u_b\cos(y_{10}-2\pi/9-2\pi/3) + u_c\cos(y_{10}-2\pi/9+2\pi/3)] \quad \text{(C14)}$$

$$x_5 = \text{sqrt}(2/3)[u_a\sin(y_{10}-2\pi/9) + u_b\sin(y_{10}-2\pi/9-2\pi/3) + u_c\sin(y_{10}-2\pi/9+2\pi/3)] \quad \text{(C15)}$$

Note: $x_3$ and $x_6$ are zero because a balanced 3-phase system is assumed

**Coordinate Transformations, cont:**

**Current Transformation (qd0 to abc):**

$$i_1 = \text{sqrt}(2/3)[y_1\cos(3y_{10}) + y_2\sin(3y_{10})] \quad \text{(C16)}$$

$$i_2 = \text{sqrt}(2/3)[y_1\cos(3y_{10}-2\pi/3) + y_2\sin(3y_{10}-2\pi/3)] \quad \text{(C17)}$$

$$i_3 = \text{sqrt}(2/3)[y_1\cos(3y_{10}+2\pi/3) + y_2\sin(3y_{10}+2\pi/3)] \quad \text{(C18)}$$

$$i_4 = \text{sqrt}(2/3)[y_4\cos(y_{10}-2\pi/9) + y_5\sin(y_{10}-2\pi/9)] \quad \text{(C19)}$$

$$i_5 = \text{sqrt}(2/3)[y_4\cos(y_{10}-2\pi/9-2\pi/3) + y_5\sin(y_{10}-2\pi/9-2\pi/3)] \quad \text{(C20)}$$

$$i_6 = \text{sqrt}(2/3)[y_4\cos(y_{10}-2\pi/9+2\pi/3) + y_5\sin(y_{10}-2\pi/9+2\pi/3)] \quad \text{(C21)}$$

Note: Again, a balanced 3-phase system is assumed

# Appendix D

## BDFM System Matrices in Simulator Notation

Matrices (L1, AA, A, L):

$$L1 = \begin{bmatrix} mp1+mp2 & 0 & 0 & 0 & 0 & 0 & mp3 & 0 & 0 \\ 0 & mp1+mp2 & 0 & 0 & 0 & 0 & 0 & mp3 & 0 \\ 0 & 0 & mp2 & 0 & 0 & 0 & 0 & 0 & 0 \\ 0 & 0 & 0 & mp8+mp9 & 0 & 0 & -mp10 & 0 & 0 \\ 0 & 0 & 0 & 0 & mp8+mp9 & 0 & 0 & mp10 & 0 \\ 0 & 0 & 0 & 0 & 0 & mp9 & 0 & 0 & 0 \\ mp3 & 0 & 0 & -mp10 & 0 & 0 & mp4+mp5 & 0 & 0 \\ 0 & mp3 & 0 & 0 & mp10 & 0 & 0 & mp4+mp5 & 0 \\ 0 & 0 & 0 & 0 & 0 & 0 & 0 & 0 & mp5 \end{bmatrix} \quad (D1)$$

$$AA = \begin{bmatrix} mp6 & mp1+mp2 & 0 & 0 & 0 & 0 & 0 & mp3 & 0 \\ mp1+mp2 & mp6 & 0 & 0 & 0 & 0 & mp3 & 0 & 0 \\ 0 & 0 & mp6 & 0 & 0 & 0 & 0 & 0 & 0 \\ 0 & 0 & 0 & mp11 & mp8+mp9 & 0 & 0 & mp10 & 0 \\ 0 & 0 & 0 & mp8+mp9 & mp11 & 0 & -mp10 & 0 & 0 \\ 0 & 0 & 0 & 0 & 0 & mp11 & 0 & 0 & 0 \\ 0 & 0 & 0 & 0 & 0 & 0 & mp7 & 0 & 0 \\ 0 & 0 & 0 & 0 & 0 & 0 & 0 & mp7 & 0 \\ 0 & 0 & 0 & 0 & 0 & 0 & 0 & 0 & mp8 \end{bmatrix} \quad (D2)$$

$$A = (-L1)^{-1}(AA) \quad (D3)$$

$$L = (-L1)^{-1} \quad (D4)$$

# Appendix E

## BDFM Machine Parameters and Basic Equations

$m_{p1} = L_{m6}$ = 6-pole magnetizing inductance (E1)

$m_{p2} = L_{l6}$ = 6-pole leakage inductance (E2)

$m_{p3} = M_6$ = 6-pole stator-to-rotor mutual inductance (E3)

$m_{p4} = L_{mr}$ = rotor magnetizing inductance (E4)

$m_{p5} = L_{lr}$ = rotor leakage inductance (E5)

$m_{p6} = r_6$ = 6-pole winding resistance (E6)

$m_{p7} = r_r$ = rotor "winding" resistance (E7)

$m_{p8} = L_{m2}$ = 2-pole magnetizing inductance (E8)

$m_{p9} = L_{l2}$ = 2-pole leakage inductance (E9)

$m_{p10} = M_2$ = 2-pole stator-to-rotor mutual inductance (E10)

$m_{p11} = r_2$ = 2-pole winding resistance (E11)

Some Basic Inductance and Flux Relationships and Definitions:

$$L_{s6} = L_{m6} + L_{l6} \quad (E12)$$

$$L_{s2} = L_{m2} + L_{l2} \quad (E13)$$

$$L_r = L_{mr} + L_{lr} \quad (E14)$$

$$\lambda_{q6} = L_{s6} i_{q6} + M_6 i_{qr} \quad (E15)$$

$$\lambda_{d6} = L_{s6} i_{d6} + M_6 i_{dr} \quad (E16)$$

$$\lambda_{q2} = L_{s2} i_{q2} - M_2 i_{qr} \quad (E17)$$

$$\lambda_{d2} = L_{s2} i_{d2} + M_2 i_{dr} \quad (E18)$$

The rotor currents, $i_{qr}$ and $i_{dr}$, may be found indirectly, either from 6-pole measurements or 2-pole measurements.

$$i_{qr} = \frac{\lambda_{q6} - L_{s6} i_{q6}}{M_6} \quad (E19)$$

$$i_{dr} = \frac{\lambda_{d6} - L_{s6} i_{d6}}{M_6} \quad (E20)$$

$$i_{qr} = \frac{L_{s2} i_{q2} - \lambda_{q2}}{M_2} \quad (E21)$$

$$i_{dr} = \frac{\lambda_{d2} - L_{s2} i_{d2}}{M_2} \quad (E22)$$

# Appendix F

## Controller Robustness With Respect to M6

Below is a summary of results for controller robustness in terms of M6:

(The operating conditions are 1500 r/min, 7.5Nm load torque, and maximum possible efficiency. V6 = 230 V, h = 0.0001, BDFMDAT5.BLK machine parameters. Simulated with RBSTCHK1.PAS, which uses RBSTSUB1.PAS. Step change in load torque, down to 6.5 Nm, as well as +100 r/min step change, are performed to test the response of the controller.)

All other machine parameters were left the same for this test.

Table F.1: M6 Robustness Data

| Error | Comments on controller behavior |
|---|---|
| +1% | Everything OK, both tests |
| +2% | Oscillatory torque response, but still works OK<br>Steady-state is smooth; ramp to 1600 r/min smooth |
| +3% | Rotor speed does not settle; goes into +/-2.2 r/min limit cycle centered at 1500 r/min. Unable to do torque step response tests. +100 r/min test OK; smooth ramp to 1600 r/min, limit cycle at 1600 r/min when "steady state" is reached |
| +4% | +/-6 r/min limit cycle at 1500 r/min. Successful ramp to 1600 r/min, but went unstable afterward -- excess flux level suspected. |
| +5% | Unable to close loop; control matrix unstable |
| -1% | Everything OK, both tests |
| -2% | Everything OK, both tests |
| -3% | Everything OK, both tests |
| -4% | Everything OK, no problems. |
| -8% | Everything still OK!<br>Interesting note: there seems to be a higher margin for error in the -% range. There is a general trend as the -% error in M6 increases: the control matrix determinant decreases, but it is still stable, and so far non-oscillatory |
| -12% | Everything still OK! |
| -16% | Torque step response slightly oscillatory; s.s. behavior is smooth. +100 r/min response good, smooth. |

Table F.1, continued:

| Error | Comments on controller behavior |
|---|---|
| -25% | Limit cycle, +/- 2.0 r/min at 1500 r/min. Aliasing seen in rotor speed display on screen. Unable to perform torque step tests. +100 rpm -- ramp smooth, +/- 2.0 r/min limit cycle at 1600 r/min |
| -30% | Limit cycle +/- 3.0 r/min (severe aliasing on screen) at 1500 r/min. Smooth ramp to 1600 r/min, +/- 4.0 r/min limit cycle at 1600 r/min |
| -35% | +/- 4 r/min limit cycle at 1500 r/min. Control matrix is highly oscillatory. +100 r/min test fell apart at 1570 r/min; machine appeared to have insufficient flux |
| -40% | +/- 5 r/min limit cycle at 1500 r/min. Control matrix looks very bad; oscillates. Was difficult to close loop successfully. +100 r/min test fell apart at 1540 r/min. (ran out of flux) |
| -45% | Unable to close loop; control matrix unstable |

It would appear that the controller is "robust" with respect to M6, with good performance in the error range of [-20% , +2%]. The controller will still function (although marginally) over [-40% , +4%].

Similar tests were performed for M2, $r_r$, and $L_{lr}$; these are summarized in Appendices G, H, and I.

# Appendix G

## Controller Robustness With Respect to M2

Below is a summary of results for controller robustness in terms of M2:

(The operating conditions are 1500 r/min, 7.5Nm load torque, and maximum possible efficiency. V6 = 230 V, h = 0.0001, BDFMDAT5.BLK machine parameters. Simulated with RBSTCHK1.PAS, which uses RBSTSUB1.PAS. Step change in load torque, down to 6.5 Nm, as well as +100 r/min step change, are performed to test the response of the controller.)

All other machine parameters were left the same for this test.

Table G.1: M2 Robustness Data

| Error | Comments on controller behavior |
|---|---|
| +2% | Unable to close loop |
| +1% | +/- 2.2 r/min limit cycle at 1500 r/min<br>+100 r/min ramp OK, smooth<br>1600 r/min: +/- 2.3 r/min limit cycle, modulated by ~ 4 Hz |
| +0.5% | OK, somewhat oscillatory response to torque step<br>ramp to 1600 r/min OK; takes long time for speed to settle to 1600 r/min |
| +0.6% | OK; oscillatory torque step; ramp OK; long time to settle to 1600 r/min |
| +0.7% | OK, oscillatory torque step; ramp OK; long time to settle to 1600 r/min |
| +0.8% | OK (long time settling); very oscillatory torque step response; ramp OK; 1600 r/min long time settling |
| +0.9% | +/- 2.0 r/min limit cycle at 1500 r/min.<br>ramp to 1600 r/min OK; settles down slowly at 1600 r/min; modulated-looking |
| -1% | Everything OK, smooth |
| -10% | Unable to close loop |
| -5% | +/- 2.3 r/min limit cycle at 1500 r/min. Control matrix has +/- 10% oscillation in determinant. Ramp OK (with extra flux boost (1.571 Volt-sec instead of 1.557 Volt-sec); +/- 2.0 r/min limit cycle at 1600 r/min |
| -3% | OK; smooth. Everything OK. |
| -4% | +/- 1.5 r/min limit cycle at 1500 r/min. Ramp to 1600 r/min OK, smooth. Settles down at 1600 r/min. |
| -3.5% | OK, smooth; everything OK. |

Table G.1, continued:

| Error | Comments on controller behavior |
|---|---|
| -3.8% | OK, smooth; oscillatory torque step response; ramp OK. 1600 r/min settles down OK. |
| -3.9% | OK, smooth; oscillatory torque step response; ramp OK. 1600 r/min settles down OK. |

The controller appears to be considerably more sensitive to error in M2 than it is to error in M6, perhaps because M2 is more directly involved with the control of the machine; it is the most direct path for the control signal to reach the rotor, from the stator.

It appears that the useful range for M2 error is [-3.9% , +0.8%], which is a total span of 4.7% of the value of M2. This is disappointing, especially after M6 gave a useful range with a 22% error span. The narrow range of 4.7% for M2 could cause some problems with getting the controller up and running, since typical instruments have a tolerance of +/- 5% full-scale.

# Appendix H

## Controller Robustness With Respect to $r_r$

Below is a summary of results for controller robustness in terms of $r_r$:

(The operating conditions are 1500 r/min, 7.5Nm load torque, and maximum possible efficiency. V6 = 230 V, h = 0.0001, BDFMDAT5.BLK machine parameters. Simulated with RBSTCHK1.PAS, which uses RBSTSUB1.PAS. Step change in load torque, down to 6.5 Nm, as well as +100 r/min step change, are performed to test the response of the controller.)

All other machine parameters were left the same for this test.

Table H.1: $r_r$ Robustness Data

| Error | Comments on controller behavior |
|---|---|
| +1% | 1500 r/min OK; slightly oscillatory torque step response; ramp to 1600 r/min OK, settles slowly at 1600 r/min |
| +2% | 1500 r/min OK; oscillatory torque step response; ramp to 1600 r/min OK; settles slowly at 1600 r/min |
| +3% | same comments as for +2% |
| +5% | same comments as for +2% |
| +10% | noticably more oscillatory torque step response; everything OK though |
| +15% | 1500 r/min OK; settles very slowly at 1500 r/min highly oscillatory torque step response; ramp OK; 1600 r/min OK |
| +20% | Limit cycle +/- 2.2 r/min at 1500 r/min; ramp OK, smooth; +/- 1.8 r/min limit cycle at 1600 r/min |
| +18% | Limit cycle +/- 2.0 r/min at 1500 r/min; ramp OK, smooth; settles slowly at 1600 r/min |
| +16% | Limit cycle +/- 1.7 r/min at 1500 r/min; ramp OK, smooth; settles at 1600 r/min |
| +15.5% | Limit cycle +/- 1.7 r/min at 1500 r/min with 2-pole flux at 1.558 volt-sec; no limit cycle with 2-pole flux at 1.568 volt-sec; ramp OK, smooth; settles at 1600 r/min |
| +15.3% | Limit cycle +/- 1.7 r/min at 1500 r/min; ramp OK, smooth; 1600 r/min OK |
| +15.2% | Limit cycle +/- 1.7 r/min at 1500 r/min; ramp OK, smooth; 1600 r/min OK |
| +15.1% | settles extremely slowly at 1500 r/min; ramp OK; 1600 r/min settles quickly |

Table H.1, continued:

| Error | Comments on controller behavior |
|---|---|
| +30% | +/- 3.2 r/min limit cycle at 1500 r/min; ramp OK; +/- 2.8 r/min limit cycle at 1600 r/min |
| +40% | +/- 6.0 r/min limit cycle at 1500 r/min; ramp OK; +/- 4.2 r/min limit cycle at 1600 r/min |
| +60% | couldn't close loop for very long; fell apart after 0.1 sec -- control matrix determinant oscillated "normally" before loop was closed but went unstable quickly after closing the loop |
| +50% | closed loop fails after 0.1 sec; control matrix determinant goes unstable |
| +45% | +/- 10.5 r/min limit cycle at 1500 r/min; very near closed-loop failure; rough but successful ramp to 1600 r/min; +/- 7.5 r/min limit cycle at 1600 r/min |
| -10% | Looks good! No limit cycles at 1500 r/min. Good, smooth torque step response; ramp OK; limit cycle +/- 0.8 r/min at 1600 r/min with 2-pole flux level at 1.570 volt-sec; when reduced to 1.560 volt-sec, limit cycle decays extremely slowly, possibly to zero, but takes too long to determine; if LC exists, it is less than +/- 0.10 r/min (at 1600 r/min) |
| -20% | 1500 r/min OK; good, smooth torque response; ramp smooth; limit cycle at 1600 r/min +/- 0.85 r/min with 2-pole flux level at 1.558 volt-sec; limit cycle is +/- 1.15 r/min with 2-pole flux level at 1.568 volt-sec<br>Note: These values of 2-pole flux level are for best efficiency at *** 1500 r/min ***, not 1600 r/min; this is excess flux for 1600 r/min. |
| -40% | Great at 1500 r/min, WONDERFUL torque step response -- no oscillation; ramp OK; 1600 r/min limit cycle is +/- 1.25 r/min with 2-pole flux level at 1.566 volt-sec; when reduced to 1.556 volt-sec, limit cycle is +/- 1.00 r/min<br>At 2-pole flux level = 1.416 volt-sec (max efficiency for 1600 r/min), limit cycle goes away; 88.323% efficiency |
| -60% | 1500 r/min OK; torque step response OK; ramp to 1600 r/min OK; limit cycle is +/- 0.90 r/min at 1600 r/min with 2-pole flux level at 1.560 volt-sec; limit cycle is at +/- 1.18 r/min with 2-pole flux level at 1.570 volt-sec; at maximum efficiency (88.301% with 2-pole flux at 1.420 V-s) there is no limit cycle |
| -80% | 1500 r/min OK; torque step response has low-frequency oscillation with about 15% overshoot; ramp to 1600 OK; limit cycle at 1600 r/min is +/- 0.76 r/min with 2-pole flux level at 1.564 V-s; when reduced to 1.414 V-s (max efficiency = 88.326%), no limit cycle, and torque step response has 15% to 20% overshoot |

Table H.1, continued:

| Error | Comments on controller behavior |
|---|---|
| -100% | When rr is assumed to be ZERO, the controller still works! 1500 r/min is OK, no limit cycle; torque step response has low-frequency oscillation, with 25-30% overshoot; ramp OK, smooth; very slow LC buildup at 1600 r/min (takes too long to find magnitude) with 2-pole flux level at 1.563 V-s; when reduced to 1.413 V-s (max efficiency = 88.323%), no limit cycle, and torque step response overshoot is about 25-30%. (7.5 to 6.5 N-m, and back to 7.5 N-m) |

It appears that the controller will still function, over an error range of [-100% , 45%], although performance may suffer somewhat. For what is considered "good" response, the useful range of the controller in terms of error in rotor resistance is [-60% , +15.1%].

This is very good news, because the variation of rotor resistance from temperature and skin-effect (as well as its difficult measurement) are no longer critical issues; the controller is quite forgiving in terms of error in this quantity.

# Appendix I

## Controller Robustness With Respect to $L_{lr}$

Below is a summary of results for controller robustness in terms of $L_{lr}$:

(The operating conditions are 1500 r/min, 7.5Nm load torque, and maximum possible efficiency. V6 = 230 V, h = 0.0001, BDFMDAT5.BLK machine parameters. Simulated with RBSTCHK1.PAS, which uses RBSTSUB1.PAS. Step change in load torque, down to 6.5 Nm, as well as +100 r/min step change, are performed to test the response of the controller.)

All other machine parameters were left the same for this test.

Table I.1: $L_{lr}$ Robustness Data

| Error | Comments on controller behavior |
|---|---|
| +1% | 1500 r/min OK; torque step OK; ramp OK; 1600 r/min settles slowly; torque step at 1600 r/min OK |
| +5% | 1500 r/min OK; torque step OK; ramp OK; 1600 r/min settles slowly; torque step at 1600 r/min OK |
| +20% | +/- 2.35 r/min limit cycle at 1500 r/min; ramp OK;<br>+/- 1.55 r/min limit cycle at 1600 r/min, la2 = 1.568Vs<br>+/- 2.20 r/min limit cycle at 1600 r/min, la2 = 1.418Vs<br>+/- 2.30 r/min limit cycle at 1600 r/min, la2 = 1.408Vs<br>(No step torque tests because of limit cycles) |
| +30% | Closed loop fell apart after 0.1 sec<br>(Control matrix determinant not stable) |
| +25% | Closed loop fell apart after 0.1 sec<br>(Control matrix determinant not stable) |
| +23% | +/- 3.80 r/min limit cycle at 1500 r/min; ramp OK;<br>+/- 2.25 r/min l.c. at 1600 r/min, la2 = 1.568,1.558;<br>+/- 4.00 r/min l.c. at 1600 r/min, la2 = 1.408 |
| +15% | 1500 r/min OK (no LC); torque response oscillatory; ramp OK; 1600 r/min OK, la2 = 1.565, torque resp. oscillatory; la2 = 1.415: 1600 r/min OK, torque response oscillatory |
| +18% | +/- 1.78 r/min l.c. at 1500 r/min, la2 = 1.558; ramp OK; 1600 r/min OK, la2 = 1.568, torque response oscillatory, la2 = 1.408: +/- 1.78 r/min limit cycle at 1600 r/min, at 7.5 Nm load torque |
| +16% | limit cycle at 1500 r/min, +/- 1.37 r/min, la2 = 1.556; no limit cycle at 1500 r/min with la2 = 1.566 (settles _very_ slowly); ramp OK; 1600 r/min OK with la2 = 1.566, torque response oscillatory; la2 = 1.416: no limit cycle at 1600 r/min, settles _very_ slowly, torque response oscillatory |

Table I.1, continued:

| Error | Comments on controller behavior |
|---|---|
| +15.9% | no limit cycle at 1500 r/min, la2 = 1.564, torque response slightly oscillatory; ramp OK; no limit cycle at 1600 r/min.<br>la2 = 1.564, torque response slightly oscillatory;<br>la2 = 1.414: no limit cycle at 1600 r/min, torque response oscillatory |
| +24% | Loop falls apart after about 0.4 seconds; control matrix determinant slowly goes unstable, oscillating |
| -5% | Unable to close loop |
| -4% | Closed loop fails after 0.1 second |
| -3% | limit cycle at 1500 r/min, +/- 2.90 r/min, la2 = 1.556<br>limit cycle at 1500 r/min, +/- 2.80 r/min, la2 = 1.566<br>ramp OK, la2 = 1.566, controller crashes at 1600 r/min at this flux level;<br>la2 = 1.406: +/- 3.45 r/min limit cycle at 1600 r/min with 7.5 Nm load torque |
| -2% | 1500 r/min OK (no LC), la2 = 1.562, very oscillatory torque step response; ramp OK; 1600 r/min OK, la2 = 1.562, highly oscillatory torque step response;<br>la2 = 1.412: +/- 1.95 r/min limit cycle at 1600 r/min, 7.5 Nm load torque |
| -1.8% | 1500 r/min OK (no LC), la2 = 1.562, very oscillatory torque step response; ramp OK; 1600 r/min OK, la2 = 1.562, highly oscillatory torque step response;<br>la2 = 1.412: 1600 r/min (7.5 Nm) settles _very_ slowly -- verge of limit cycle; highly oscillatory torque step response |
| -1.9% | 1500 r/min OK (no LC), la2 = 1.556, very oscillatory torque step response; ramp OK (la2 = 1.566);<br>1600 r/min OK, la2 = 1.556, very oscillatory torque step response; la2 = 1.416: limit cycle, +/- 1.80 r/min at 1600 r/min with 7.5 Nm load torque |

It appears that the closed-loop error limits for $L_{lr}$ are in [-3% , +23%], with an interval length of 26%.

The "useful" range (no limit cycles) of error limits for Llr appears to be [-1.8% , +15.9%] (interval length of 17.7%). It is hoped that the rotor laminations may be designed, built, and measured with with sufficient accuracy/precision.

# Appendix J

## BDFM Simulation Package: Features and Limitations

The heart of the program is an RK-4 algorithm, which is used to integrate the BDFM system differential equations, in the rotor reference frame. The rotor reference frame is used because it provides constant (time-invariant) coefficients for the differential equations. As discussed earlier, any choice of reference frame will have time-varying forcing functions (voltages) and state variables (currents), but only the rotor reference frame will provide constant differential equation coefficients. This is all that is required for straightforward RK-4 integration of the equations. Of the several different methods available for integrating the differential equations, RK-4 was chosen, mainly because it is well-established and simple to implement. Linear and non-linear systems may both be simulated with RK-4, as long as their equations are not "stiff"; that is, the ratio of the largest to smallest time constants in the system is reasonably small, on the order of perhaps 10 to 100 at the most. Other methods must be applied for the solution to "stiff" systems; these will not be discussed here.

It has been found that the RK-4 simulation algorithm, with a fixed time-step, is sufficient to accurately simulate the BDFM system. This has been verified in several ways; with a good choice of integration time step, further reductions in time-step yield more accurate yet consistent results. Depending on machine parameters, an integration step size as large as 3 ms may be used to simulate the BDFM in the open-loop, although accuracy suffers; this mode is used mainly for speed, to quickly set up the machine to a desired operating point. A "good" general-purpose integration step size is 1 ms for the BDFM in the open-loop; this is roughly an order of magnitude smaller than the smallest time constant and yields adequate resolution for the constant 60 Hz excitation of the 6-pole windings. The program has

some built-in checks and balances; displayed values of electrical torque, load torque, shaft speed, power, and efficiency provide insight into the consistency of the calculated quantities. Integration error (as seen in inconsistencies in the named quantities) is acceptably low with a 1 ms time step, on the order of 1 percent; this allows fast open-loop simulation with reasonably reliable results. If higher accuracy is desired, the integration step size may be reduced, during simulation, to 0.5 ms, 0.2 ms, or to 0.1 ms or lower. It has been found that 0.1 ms provides enough accuracy for even the most critical needs (less than 0.1% error), and further reductions in step size only cause the simulations to run much slower, with diminishing returns; truncation error may also increase. In the closed-loop, all simulation must be done with 0.1 ms step size or lower, because of the 1 ms switching period of the controller. Closed-loop simulations are slow and time-consuming because of this, although the use of a 486/50 could yield a 5- to 10-fold increase in speed over the 386/20 used in this research.

The BDFM simulation packaged developed for this project, written in Turbo Pascal 6.0, is interactive and graphical in nature. The BDFM was originally simulated in Fortran [12], using the reduced-order model described in the introduction. While this program provided some important information, it lacked a graphical display, and furthermore was non-interactive. This inspired the development of the simulator described here, to gain intuitive insight into machine operation.

The graphical display of the simulator is centered around the shaft speed of the machine; this is the quantity being controlled. The behavior, or "personality" of the machine is readily apparent by observing the speed response of the machine to various disturbances. Other state variables may also be plotted if desired, but they are generally of secondary importance and are superimposed over the speed display. Figure J.1 shows a typical screen, with the machine operating in the open-loop. The speed display is always active.

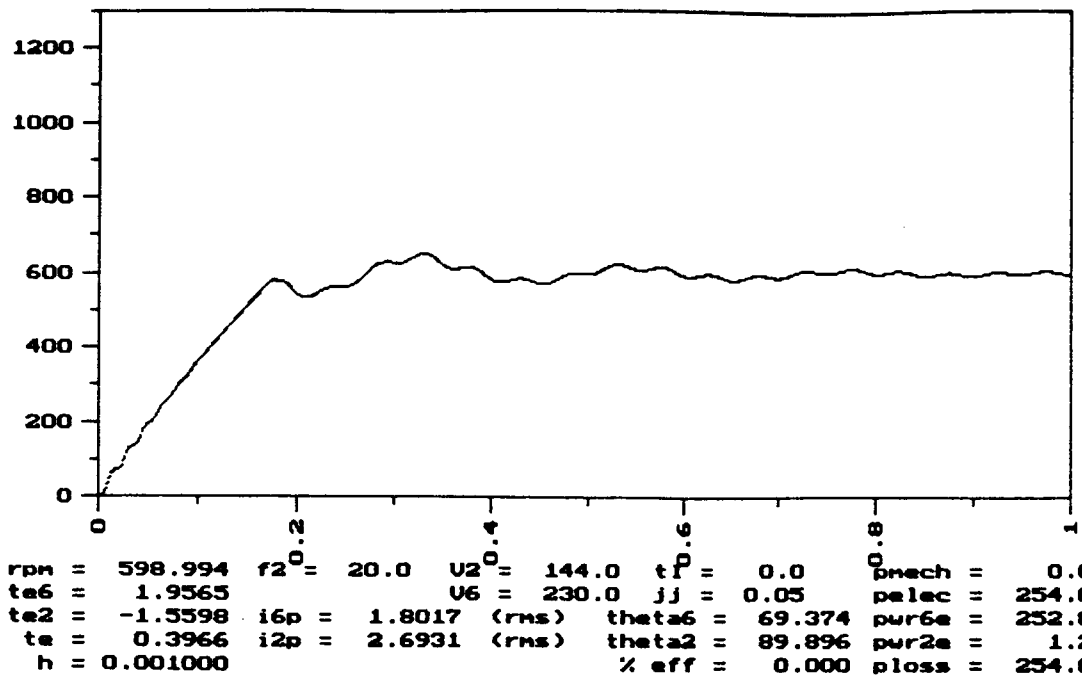


Figure J.1: Simulator Display in Open-Loop Mode

Time-scaling is fixed throughout the execution of the program but may be user-chosen by changing the value in the input file. Vertical scaling (of shaft speed) is changeable at any time, with the use of "zoom-in", "zoom-out", "offset-up", and "offset-down" options. Vertical scaling for the other state variables is more limited; the "zoom" feature is not present. Only pure scaling factors (without offsets) are allowed.

Outside the plotting screen border, other critical quantities of the machine are displayed in numeric format. These numeric displays (the dynamic quantities) are updated every time a new pixel is plotted on the screen, which is typically every millisecond. (To be more precise, 1000 times per screen width.) The numeric displays are done using Turbo Pascal graphics characters; these require considerable time and slow down the simulation process, by up to a factor of 2 or more. To get around this, these displays were designed to be toggled on or off by the user. In this way, the fastest simulations are possible, and the numeric data may be viewed when needed.

The program's interactiveness originates from its wide selection of "hot keys", which can be used to change simulation parameters, program parameters, or display parameters. The hot keys, and their functions, are listed below.

Table J.1: Simulator Hot-Keys and Descriptions

| Hot Key | Function |
|---|---|
| <space> | freeze/unfreeze simulation |
| q,Q | quit |
| m,M | "more" -- simulate another screen |
| t,T | toggle torque display on/off |
| i,I | toggle current display inst/rms/off |
| p,P | toggle phase-angle/power-factor display |
| r,R | toggle r/min display on/off |
| Z | zoom out vertically, for speed display |
| z | zoom in vertically, for speed display |
| PageUp | offset vertical speed display, higher r/min |
| PageDn | offset vertical speed display, lower r/min |
| x,X | open/close data output to disk file. Turn this on, ONLY WHEN NECESSARY, as it will fill up disk space, fast! |
| b,B | back-up -- freezes simulation, allows user to use left, right arrow keys to select previous operating point, for crash recovery. Works only for open-loop; closed-loop back-up has bugs. |
| right | select large value changes |
| left | select small value changes |
| up | higher speed; lower f2 |
| down | lower speed; higher f2 |
| 7 | increase 6-pole voltage |
| 1 | decrease 6-pole voltage |
| 9 | increase 2-pole voltage (open loop)<br>increase 2-pole flux level (closed loop) |
| 3 | decrease 2-pole voltage (open loop)<br>decrease 2-pole flux level (closed loop) |
| 8 | increase load torque |
| 2 | decrease load torque |
| + | increase rotor moment of inertia<br>(to simulate loads, or to temporarily stabilize machine to obtain an operating point) |
| - | decrease rotor moment of inertia<br>(to temporarily stabilize machine to obtain an operating point; for simulation speed only; user must return to proper value after machine settles) |
| 4,5,6 | "kick" system with 2-pole phase changes<br>4 --> -90 degrees; 6 --> +90 degrees<br>5 --> 180 degrees (large value changes)<br>4 --> -5 degrees; 6 --> +5 degrees<br>5 --> 180 degrees (small value changes)<br>This feature no longer used, but still exists in simulator program. May be removed. |
| H | increase integration step size to next convenient level (1,2,5 ratios) |
| h | decrease integration step size to next convenient level (5,2,1 ratios) |

Table J.1, continued:

| Hot Key | Function |
|---|---|
| V | "viewstates" on -- display other state variables, superimposing them on top of speed display This also causes converter output to change only once per control update period, giving it a sample-and-hold output waveform. Controller calculations are also made, but loop remains open. Integration step size MUST be 0.1 ms or less to use this feature. |
| v | Turns "viewstates" off. Controller must be turned off first, or it will "crash". |
| C | Close the loop, activate controller. "Viewstates" MUST be turned on before closing loop, or controller will crash. |
| c | Open the loop, deactivate controller. Simulator reverts to open-loop operation, with "viewstates" still turned on. Open-loop voltage command for converter is likely to be of incorrect phase; BDFM will most likely crash. Future versions of program will measure closed-loop phase angle for smooth transition to open-loop. |
| E | "Efficalc" on. This forces the simulator to do a more accurate, window-averaged calculation of electrical torque and efficiency, for display, with "viewstates" on. Otherwise, fluctuations in instantaneous quantities will appear, and the true averages will be incorrectly displayed. |
| e | "Efficalc" off. This reduces the calculation load on the simulator, increasing speed. |
| l,L | capture current value of "Lambda-2", the 2-pole flux level. This must be done before loop is closed (after "V" but before "C"), so the controller will have a command value for 2-pole flux level. Best to wait for system to settle for 1/2 second or so, after pressing "V", before pressing "l" or "L". |
| Insert | select next state variable for display |
| Delete | select previous state variable for display |
| Home | compress vertically, for state variable display |
| End | magnify vertically, for state variable display (not the same as zoom out/in; no offsets available) |
| d,D | toggle state variable display on/off; displays index number of state variable being plotted Future versions will leave this ON as long as "viewstates" = on; also, name of state variable will be displayed, for better clarity. |

One important feature of the program is the ability to accept machine parameters from an external data file. In this way, an infinite number of different machines may be simulated by the same program, as long as they have the same 6-pole, 2-pole structure. The external data file must adhere to a very strict syntax, and it is highly recommended that an input file known to work properly simply be edited, changing only the machine parameter

values. This file contains the machine parameters used for this research and is of the proper format; it is thus a good foundation to start with when simulating other machines. The input data file also contains some simulator parameters, such as default 6-pole voltage (line-to-line), default integration step size (choices are given), and time scaling for the graphic display, which is not changeable during program execution.

The program is capable of exporting simulation data to text files, for detailed analysis with a spreadsheet or signal processing software. The data written include 6-pole, 2-pole, and total torque; 2-pole flux level; 6- and 2-pole voltages and currents (abc). Data is recorded every 1 ms.

The anti-crash recovery system is a valuable addition to the program for open-loop simulation. Operating points frequently require significant simulation time to reach, and any mistake such as adding excess load torque or changing speed too quickly may result in a "stall" of the machine, losing the operating point. The anti-crash recovery system saves all state variables of the machine, every 1/10 of a screen width, for a total of 5 sets of data (total of 1/2 screen width). In the event of a BDFM crash, the simulation is stopped, and the user is able to "back-up" to the desired time before the crash occurred, moving a graphic cursor on the screen. When the user makes a choice, the simulation re-starts from the selected operating point, as if a crash had never occurred.

The simulator, like any other software, has its limitations and fills only a small niche in electric machines research. The RK-4 integration step-size, although user-selectable at any time, is fixed. The main advantage of this is program simplicity (lower susceptibility to "bugs"). Screen updates, keyboard strobes, and data exports are kept uniformly spaced in time because all use the total elapsed time, t, as a master "clock". The disadvantage of fixed step size is that the simulation speed and accuracy are somewhat compromised; to assure accuracy, a small step size must be

selected, slowing the simulation. The simulation continues to run slowly, even when small time steps are no longer necessary, until the user selects a larger step size. Variable step-size integration could facilitate accurate simulation of the space-vector PWM converter model, by providing the necessary time resolution; this, however, makes master "clock" management much more complicated. Another limitation of the simulator is that it will simulate only 6-pole, 2-pole machines. The differential equations are set within the program sourcecode, and machines with different geometries will require significant changes and program re-compilation. Finally, higher-order effects of the BDFM are not simulated. The B-H curves of the stator and rotor magnetic cores are nonlinear, but the simulator uses only a linear model. Harmonics generated by stator/rotor slots and winding distribution are ignored. Skin-effect of the conductors, particularly in the rotor, is also neglected. Although simulation accuracy may be improved, adding these models into the simulation package would slow it down excessively and defeat its purpose; intuitive feel would be lost. If simulations requiring a more detailed model are necessary, refer to [19].

Throughout the development of the simulation package, the sourcecode has been modified numerous times, for the addition of features and the correction of programming errors (debugging). The latest version currently in use for simulation of closed-loop BDFM performance is BDFMC41Y.PAS. The name of the file represents "BDFM Controller, Revision 41, sub-revision Y". Large changes, particularly those involving new features, are generally represented by an increase in the revision number, while small changes due to debugging are represented by a letter following the number. All sourcecode files end in ".PAS" because they are written in Turbo Pascal (Version 6.0).

The main program makes use of numerous subroutines, many of which are included in an external file called BDFMSUB1.PAS. The name of the file merely represents "BDFM Subroutines, Revision 1". The subroutines in this file are mainly graphics subroutines and others which are unlikely to be

changed during the development and debugging of the control algorithm. The file BDFMSUB1.PAS also makes use of some external subroutine files, and included among these are MATRIX1.PAS (from Borland's Numerical Methods Toolbox for Turbo Pascal), FINDTICK.PAS, and SIGFIG.PAS. The first is used for the required matrix inversions; the latter two are used to determine the spacing of major and minor tickmarks in the plotting screen, and to "clean up" the numerical representations of the tickmark labeling.

Another series of simulator programs has been developed, toward the end of the project, to verify the correctness of the controller code to be placed into the DSP. This series is referred to as DSPSIMxx.PAS, where the "xx" refers to the revision number. The DSPSIMxx.PAS series was developed concurrently with the BDFMCxxx.PAS series; changes in one were reflected by similar changes in the other. The DSPSIMxx.PAS series uses the same subroutine module, BDFMSUB1.PAS.

To test the controller for robustness, the simulator program required some moderately extensive modifications. These modifications were specific to this task, so a new series name was selected, RBSTCHKx.PAS. Only one revision number of this program currently exists; it is RBSTCHK1.PAS. The subroutine module also required some similarly large modifications; it was renamed to RBSTSUB1.PAS.

All programs mentioned above use the same input data file, which can have any name that the user chooses. The data file used throughout this study is named BDFMDAT5.BLK; it contains the machine parameters of the laboratory prototype. In the early stages of program development, the format of this data file went through some changes, and the number "5" in the filename represents the 5th format revision of the file. It has remained unchanged for most of the history of the BDFMCxxx.PAS series. Since the user is free to select any filename for the machine parameters, any changes in the required format are reflected in the program sourcecode, with the current revision number and a sample file included (as comments).